OCEANS AND ATMOSPHERE
www.csiro.au

Air Quality Modelling of Smoke Exposure from the Hazelwood Mine Fire

Kathryn Emmerson, Fabienne Reisen, Ashok Luhar, Grant Williamson and Martin Cope

December 2016

Client: Monash University

UNIVERSITY of TASMANIA | MENZIES Institute for Medical Research

Citation

Emmerson, K.M., Reisen, F., Luhar, A., Williamson, G., Cope, M.E. 2016. Air quality modelling of smoke exposure from the Hazelwood mine fire. CSIRO Australia.

Copyright and disclaimer

Important disclaimer

Contents

Figures

Tables

Executive summary

The Hazelwood coal mine fire began on February 9th 2014 and burned for 45 days.

A preliminary smoke tracer study, conducted by CSIRO in April 2015, showed most towns within a 30km radius of the mine fire were exposed to high concentrations of smoke. The highest concentrations of smoke from the fire occurred when the winds were blowing from a south westerly direction. The preliminary study was conducted in the absence of smoke emission rates for the fire and also was not able to resolve strong concentration gradients for locations (such as Morwell) immediately adjacent to the mine.

In the current study our smoke exposure modelling has been refined through the use of quantitative estimates of hourly emission rates of various species based on parameters such as how much coal was burned using maps of the area burned drawn by the Country Fire Authority and estimated emission factors. Additionally we have used both a high-resolution near-field model and a regional scale model in order to better resolve smoke concentration gradients across the impacted areas in the Latrobe Valley – Gippsland region.

The high resolution near-field concentration predictions were generated using CSIRO's The Air Pollution Model (TAPM) in order to properly resolve the smoke plume around Morwell within a domain of 10 km × 10 km. The coal fire area was represented by a number of ground-level point sources each 100 m apart. Particulate matter with an aerodynamic diameter of 2.5 microns or less ($PM_{2.5}$) and carbon monoxide (CO) from the fire were treated as tracer species (i.e. no chemistry acted upon them) within the selected domain and dispersed using TAPM predicted meteorology. Hourly $PM_{2.5}$ concentrations of up to 3700 $\mu g\ m^{-3}$ and CO concentration up to 60 ppm were predicted in the early phases of the fire at Morwell South. These predictions for Morwell East were 2200 $\mu g\ m^{-3}$ and 35 ppm, respectively. Direct comparisons between the model and observations showed that TAPM predicted the correct magnitude, but did not always predict observed temporal maxima at the same time. However, when concentrations are unpaired in time TAPM simulates the concentration distribution around Morwell satisfactorily. This result demonstrates that the assumptions made in the modelling, especially in the emissions methodology, are realistic.

The fine-scale modelling showed that residents of Morwell were exposed to the greatest number of breaches of the $PM_{2.5}$ air quality standard, exceeding it on 23 days at Morwell South and 12 days at Morwell East locations out of a total 45 days the fire burned. There were 5 breaches of the $PM_{2.5}$ limit at Traralgon. The 8-hour limit for CO was exceeded 7 times at Morwell South.

The second modelling system conducted full chemistry simulations. The CSIRO Chemical Transport Model (CTM) coupled with the CCAM meteorological model was used to predict the exposure of residents living in towns across the Latrobe Valley, such as Sale, chosen as the control group for the long term Hazelwood health study.

Regional modelling of background concentrations showed $PM_{2.5}$ levels at 6 $\mu g\ m^{-3}$ in Morwell. This demonstrates the level of $PM_{2.5}$ that would have been present in Morwell if the Hazelwood mine fire had not taken place. It includes the contribution from all anthropogenic sources and any wildfires occurring in Victoria during February and March of 2014. Likewise, background CO concentrations were 0.07 ppm. The air quality in the closest towns to the mine was returned to background levels after March 12th 2014.

Inclusion of the mine fire in the CTM resulted in peak concentrations of up to 2000 $\mu g\ m^{-3}$ for $PM_{2.5}$ at Morwell South. In the absence of measurements at this time, this predicted concentration is reasonable as fire activity was maximum during the early phases of the fire. The magnitudes of the predicted $PM_{2.5}$ and CO as compared to the observations demonstrates that the emission rates calculated in the first exercise are reasonable.

Outside of Morwell $PM_{2.5}$ concentrations decreased rapidly. There were 3 breaches of the $PM_{2.5}$ air quality standard at Churchill, and 2 breaches at Moe and Traralgon. There were no breaches of the CO air quality standard (9ppm as an 8 hour average) outside of Morwell.

The regional model also predicted low concentrations of $PM_{2.5}$ and CO for the exposure control population at Sale. The peak hourly $PM_{2.5}$ concentration predicted at Sale was 17 $\mu g\ m^{-3}$ on 10th February, whilst peak CO was 0.46 ppm on 22nd February. There were no breaches of either air quality standards predicted at Sale during the mine fire.

1 Introduction

On 9th February 2014, sparks from a nearby grass fire ignited coal within the Hazelwood mine, Latrobe Valley, Victoria. The fire burned for 45 days, sending smoke across the nearby town of Morwell with a population of approximately 14,000. Whilst the health effects due to smoke exposure from the mine fire are not currently known, residents complained of smoke inhalation, loss of visibility and amenity. An inquiry into the incident paved the way for the Hazelwood Mine Fire Health Study (HMFHS), which brings together health professionals, epidemiologists and air quality specialists (http://hazelwoodhealthstudy.org.au/). The HMFHS commissioned an initial exposure assessment in order to assess how far the smoke travelled, and thus whether a suitable control population existed within the Latrobe Valley for the purposes of a long term health study. Emmerson et al. (2015) used the CSIRO chemical transport model (CTM) to predict concentrations of a smoke tracer emitted from Hazelwood across the Latrobe Valley. A smoke tracer was used as there were no initial estimates of how much coal was burned, or which chemical species the Hazelwood coal emitted. Figure 1 shows the calculated dispersion of smoke by the CTM during February and March 2014.

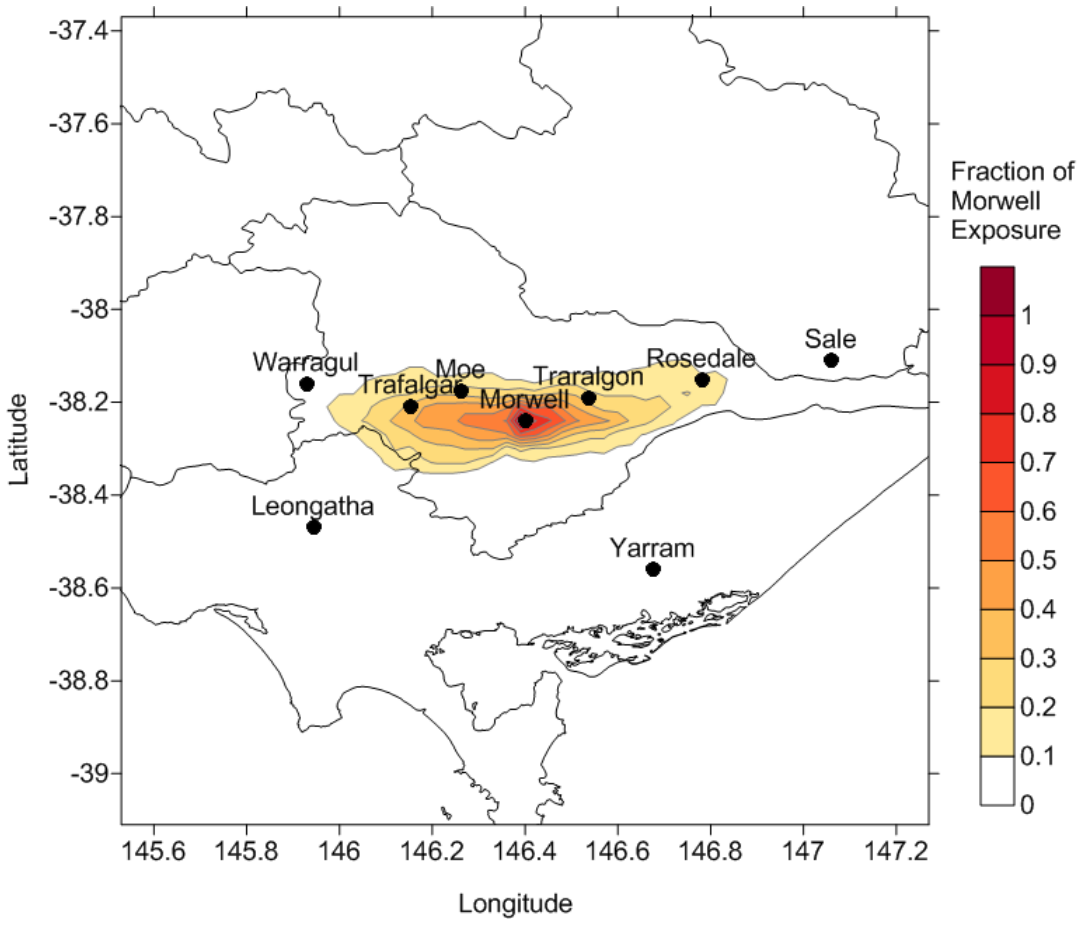

Figure 1 Modelled smoke exposure of populations in Latrobe valley towns during the period of the Hazelwood mine fire.

The units of Figure 1 are in terms of smoke exposure relative to exposure at Morwell (i.e. assume that Morwell =1). The pattern of dispersion was in an east-west direction, mirroring the geography of the Latrobe Valley. Nearby towns of Traralgon, Moe and Rosedale experienced a much lower fraction of smoke than was experienced at Morwell, and the town of Sale was chosen as the control population.

The previous report was an initial estimate of exposure; the current report will predict concentrations of smoke in terms of criteria pollutant species such as carbon monoxide (CO) and particulate matter with an aerodynamic diameter of 2.5 microns or less ($PM_{2.5}$). An assessment of how much coal was burnt, and exactly what chemical species were emitted by the mine fire has been estimated. These estimates have been checked via very high resolution near-field modelling and compared to concentrations of pollutants measured at nearby air quality monitoring stations in Morwell, Churchill, Moe and Traralgon. Regional modelling is then undertaken to assess concentrations of CO and $PM_{2.5}$ across Victoria.

Outline of what this report is about:

- Finalising the emission estimates for the mine fire, by calculating a bottom-up mass constraint on the total amount of coal burnt. The mass of coal burned each day has been calculated from daily maps provided by the Country Fire Authority.
- Using Global Fire Assimilation System (GFAS) smoke estimates for wildfires in Australia at 10km resolution, but using a higher resolution locally produced smoke emissions inventory for Victorian wildfires.
- Conducting regional background air quality modelling which does not include the Hazelwood mine fire emissions. This will predict the magnitudes of concentrations of CO and $PM_{2.5}$ usually experienced by people in the Latrobe Valley.
- Near-field modelling down to 100m resolution; necessary because the resolution of the regional model is too coarse to elucidate the smoke exposure of residents in nearby Morwell. This means that the mine fire in the regional model is contained in the same or adjacent grid cell, thus the effects cannot be resolved properly. The innermost near field model domain is 10 km by 10 km
- Regional modelling (background + fire); this will predict concentrations experienced by residents in towns outside the near-field grid, across the whole of Victoria.

2 Emissions

One of the major challenges for accurately determining exposures lies in the estimation of emissions from the Hazelwood mine fire. Emissions are generally estimated by the following generic equation:

$$E_x = \int EF_x \, dM_c . dt \qquad (1)$$

Where E_x is the amount of species x emitted in time dt,

EF_x is the molar emission factor of species x expressed as g of species x per kg of fuel carbon burned, and

dM_c is the mass of fuel carbon consumed per unit time

These variables have been populated by comparing values from the literature with constraints placed on the total emissions by air quality measurements conducted at nearby monitoring stations.

2.1 Emission factors for fires from the literature

Emissions from combustion of any biomass fuel are affected by several factors including fuel characteristics (e.g. structure and arrangement, size, moisture content, composition) and combustion conditions (e.g. oxygen availability, temperature). Combustion efficiency (CE) is a key factor as it determines the extent to which fuel carbon is oxidised. Emissions of most organic compounds and particles increase with decreasing CE. For biomass fuels, fine fuels (e.g. leaf litter, grass and twigs) and dry fuels tend to burn at high CE resulting in comparatively low emissions of organic gases and aerosols. On the other hand, larger fuels (branches and logs) as well as below-ground fuels (e.g. peat, organic soil) burn less efficiently and emit substantially more organic species. Combustion of biomass proceeds through different stages (i.e. thermal degradation, oxidation of volatiles in flaming combustion, char oxidation in smouldering combustion), each with different chemical processes that result in different emissions (Andreae and Merlet, 2001). Within a fire these processes occur simultaneously and are interlinked.

Coal has a high carbon content (65-70% for Victorian lignite brown coal), high density and burns under a typical fuel-rich combustion process. This means that combustion is less efficient resulting in greater yields of incomplete combustion products such as CO, benzene and polycyclic aromatic hydrocarbons (PAHs). Fire spread is also slow compared to fine fuels but coal burns at higher temperatures (peak temperatures of ~1,000°C) than those typically observed for smouldering combustion (500-700°C) (Rein et al., 2008). Therefore burning of coal can be accompanied by flames near the open surface (Rein, 2016).

A literature review has shown that only a limited amount of research has focused on emissions from coal fires. Previous research studies have investigated exhaust gases in vents from underground coal mine fires in the US (Engle et al., 2012; Hower et al., 2009; Hower et al., 2013; O'Keefe et al., 2010; O'Keefe et al., 2011; Hower et al., 2011) and South Africa (Pone et al., 2007). While these studies provide some information on the potential amount of gases emitted during coal mine fires, the combustion conditions are significantly different to an open-cut coal mine fire, especially in terms of available oxygen. This is likely to result in significantly different emission rates of pollutants. Currently available data in the literature on emission characterisation from open-cut coal mine fires are very limited.

The current understanding of the combustion of solid fuels such as Victorian brown coal has been focused on burning in furnaces and industrial processes. The emission factors derived from these studies are not appropriate because unlike the Hazelwood mine fire, these devices are designed to maximise carbon oxidation with near complete combustion of gaseous organic species and carbon containing particles. Furthermore experience with open burning of biomass (vegetation) suggests that the combustion process itself is a greater contributor to emissions than the composition of the fuel (Meyer et al., 2012). In particular there is a significant difference between emissions from biomass fuel burned in laboratory conditions to fuel burned in more field-like conditions. This is also true for coal: conditions of heating rate, temperature, and oxygen availability are known to be significant factors in determining the quantity and speciation of the combustion products. While many laboratory studies have attempted to quantify the impact of these variables on the products of pyrolysis and combustion, the complex conditions experienced in an open-cut mine fire mean that interpretation of such studies needs to be assisted by real-world data.

However in the absence of direct measurements, some guidance can be derived from the literature. In fact numerous research studies on biomass burning have provided a large data set of emission factor (EF) measurements which have been reviewed in Akagi et al. (2011). In this review a comprehensive tabulation of EFs for known species emitted during biomass burning is presented with EFs being categorised into 14 fuel or vegetation types. Furthermore a study by Tian et al. (2008) provides published data for combustion of anthracite and bituminous coals in a fire pit, while Bond et al. (2002) provides data on particle emissions from residential coal burning.

2.2 Emission factors – Hazelwood mine fire

Emission factors can also be assessed by using air quality measurements downwind of a fire. Table 1 provides a summary of the air quality measurements at the Morwell South Air Monitoring Station (AMS) during the Hazelwood mine fire that are relevant for emissions calculations. It should be noted that air quality measurements started 10 to 22 days after the start of the Hazelwood mine fire.

Table 1 Air quality measurements at the Morwell South AMS during the Hazelwood mine fire.

Pollutant	Instrument	Frequency	Period
$PM_{2.5}$	Beta attenuation monitor (BAM)	Continuous	19/2/14-1/5/15
PM_{10}	HiVol with PM_{10} inlet	24h (6 day cycle)	26/2/12-1/5/15
Size-fractionated PM	MOUDI (12 stage 0.056-10 µm) Hi Vol Moudi (6 stage 0.25-10 µm)	2-4 days	3/3/14-21/3/14
CO	IR absorption spectrometer	Continuous	19/2/14-1/5/15
NO_2, NOx SO_2	Chemiluminescence Pulsed fluorescence spectrometry	Continuous Continuous	6/3/14-1/5/15 19/2/14-1/5/15
VOCs	Canisters Radiello (passive)	24h (5 samples) 7-day sample	26/2/14-14/3/14 26/2/14-1/5/15

2.2.1 CARBON MONOXIDE

Given a modified combustion efficiency (MCE), it is possible to estimate CO EFs as follows:

$$EF(CO) = (1 - MCE) \times \left(\frac{MW_{CO}}{12}\right) \times CC \times BEF \qquad (2)$$

Where MCE is the modified combustion efficiency defined as $\frac{\Delta CO2}{\Delta CO2+\Delta CO}$

MW_{CO} is the molecular weight of carbon monoxide,

CC is the carbon content of coal (approximately 0.68 for Victorian lignite coal), and

BEF is the burning efficiency, being the mass proportion of the mass of combusted fuel that is volatilised in a fire (assume 95% based on a mineral content of brown coal of 5%).

From the published literature data it is assumed that MCE ranges between 0.75 (smouldering combustion) and 0.95 (flaming combustion). The calculated EF for CO as a function of MCEs are presented in Table 2. Considering the structure and high carbon content of the coal, coal is most likely consumed by a less efficient smouldering combustion. Therefore the most likely EFs for CO are presented in bold and range from 151 to 301 g kg^{-1} with a median of 226 g kg^{-1} ± 75 g kg^{-1}.

Table 2 Estimated range of CO emission factors as determined by Eq.2.

MCE	EF (CO) (g kg^{-1})
0.75	377
0.80	**301**
0.85	**226**
0.90	**151**
0.95	75

To determine EFs for specific pollutants, enhancement ratios (ER) were calculated using measured concentrations of pollutants from the Morwell South AMS downwind of the coal mine fire. The ERs can be calculated by either taking the ratio of the enhancement of a species of interest above background to the enhancement of a stable representative plume tracer, in this case CO or by determining the linear regression slope between a species of interest and the plume tracer, assuming that measurements are well-correlated.

The following equation is used to convert ERs into EFs:

$$EF_x = ER_{x/y} \times \frac{MW_x}{MW_y} \times EF_y \qquad (3)$$

Where $ER_{x/y}$ is the emission ratio of species x relative to the reference species y,

MW_x and MW_y are the molecular weights of species x and the reference species y, and

EF_y is the emission factor of the reference species.

In the case of the Hazelwood mine fire, CO is used as a reference species.

2.2.2 $PM_{2.5}$

Figure 2 shows the relationship between $PM_{2.5}$ and CO concentrations measured at Morwell South AMS. The left panel shows the mean hourly concentrations measured at Morwell South AMS between 19th February and 25th March 2014, while the right panel shows averaged concentrations from 25 identified plume events. Plume events were defined as time periods when concentrations of CO and PM2.5 were well above their corresponding background levels. The large scatter is likely due to the difference in combustion conditions, which was a mix of flaming and smouldering combustion. Previous studies have shown a strong relationship between EFs of particles and MCE. The gradient of the $PM_{2.5}$ to CO relationship increases with CO concentrations from 34 g $PM_{2.5}$ (kg CO)$^{-1}$ at CO concentrations below 8 mg m^{-3} to 101 g $PM_{2.5}$ (kg CO)$^{-1}$ at CO concentrations > 8 mg m^{-3} (Figure 2).

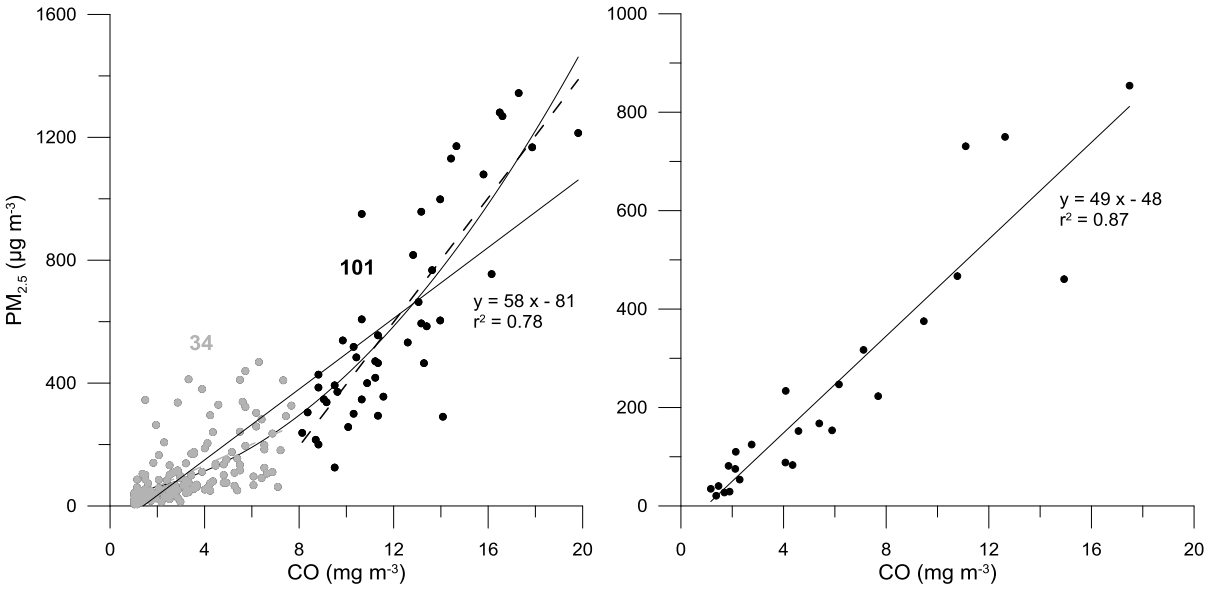

Figure 2 Relationship between $PM_{2.5}$ and CO concentrations measured at Morwell South AMS; left: mean hourly $PM_{2.5}$ and CO concentrations when CO > 1ppm (black = CO > 8 mg m^{-3}. Grey = CO < 8 mg m^{-3}); right: averaged $PM_{2.5}$ and CO concentrations for 25 identified smoke plume events.

Using the ERs and the EF for CO, EFs for $PM_{2.5}$ can be calculated as follows:

$$EF(PM_{2.5}) = EF(CO) \times ER \qquad (4)$$

Where ER is the emission ratio of $PM_{2.5}$ relative to CO (in g $PM_{2.5}$ (kg CO)$^{-1}$) and is estimated from the linear regression slope between $PM_{2.5}$ and CO measurements (see Figure 2)

Table 3 presents the estimated range of $PM_{2.5}$ emissions factors for a range of MCE and ERs appropriate to the Hazelwood mine fire.

Table 3 Estimated range of $PM_{2.5}$ EFs (g kg^{-1} coal) determined by Eq 3 and 4.

MCE	EF ($PM_{2.5}$) (g kg^{-1})			
	ER($PM_{2.5}$/CO) = 30	ER($PM_{2.5}$/CO) = 45	ER($PM_{2.5}$/CO) = 60	ER($PM_{2.5}$/CO) = 75
0.75	11.3	17.0	22.6	28.3
0.80	9.0	**13.6**	**18.1**	22.6
0.85	6.8	**10.2**	**13.6**	17.0
0.90	4.5	**6.8**	**9.0**	11.3
0.95	2.3	3.4	4.5	5.7

The most likely EFs for $PM_{2.5}$ (based on probable MCE and estimated ERs) are presented in bold and range from 7 to 18 g kg^{-1} with a median of 12 g kg^{-1} ± 4 g kg^{-1}.

2.2.3 SO_2 AND NO_2

Figure 3 shows the relationship between SO_2 and CO concentrations measured at Morwell South AMS. SO_2 measurements started on 20 February 2014. During the measurement period 18 plume events were identified when CO and SO_2 measurements were well above their corresponding background concentrations. The left panel shows averaged concentrations from the 18 identified plume events, while the right panel shows the mean hourly concentrations measured at Morwell South AMS between 19th February and 25th March 2014. Ambient measurements of SO_2 and CO are moderately correlated (r^2 = 54) and this may reflect the non-suitability of CO as a reference species. In fact while SO_2 is predominantly emitted during flaming combustion, CO is predominantly formed during incomplete combustion. Carbon dioxide (CO_2) would be a more suitable reference species for species emitted during flaming combustion, but no measurements of CO_2 were made during the Hazelwood mine fire.

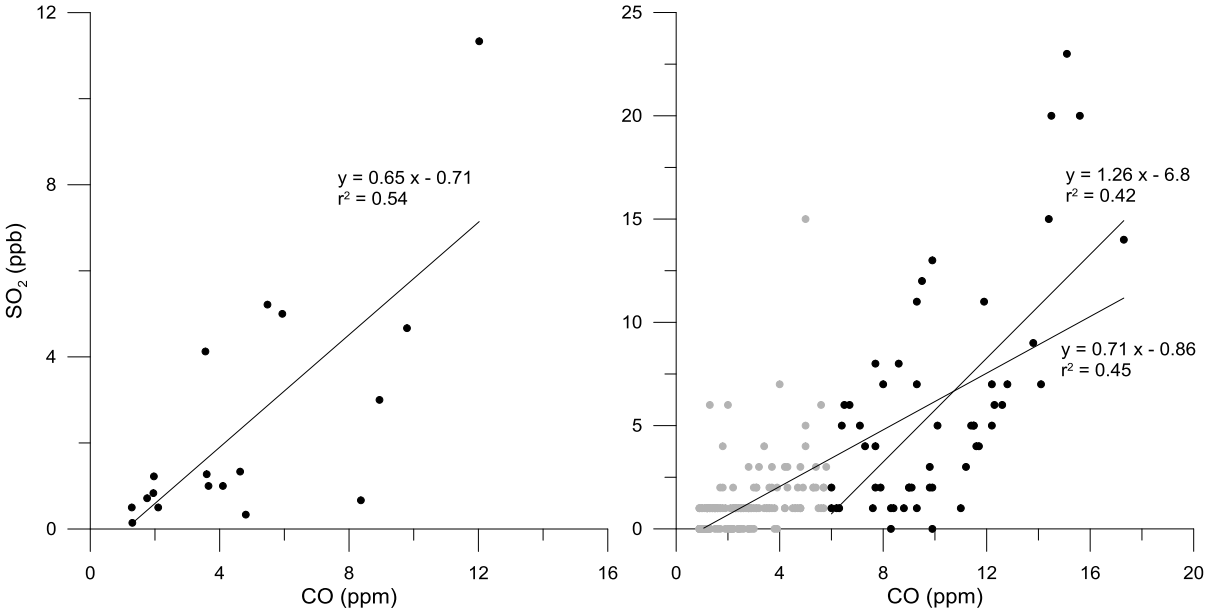

Figure 3 Relationship between SO_2 and CO concentrations measured at Morwell South AMS; left: averaged SO_2 and CO concentrations for 18 identified smoke plume events; right: mean hourly SO_2 and CO concentrations when CO > 1ppm (black = CO > 6 ppm, grey = CO < 6 ppm).

Table 4 presents the estimated range of SO_2 emissions factors for a range of MCE and ERs determined from the linear regression slope of the correlation between SO_2 and CO. The most likely EFs for SO_2 (based on probable MCE and estimated ERs) are presented in bold and range from 0.21 to 0.48 g kg^{-1} with a median of 0.34 g kg^{-1} ± 0.10 g kg^{-1}.

Table 4 Estimated range of SO_2 EFs (g kg^{-1} coal) determined by Eqs 3 and 4.

MCE	EF (SO_2) (g kg^{-1})			
	ER(SO_2/CO) = 0.50	ER(SO_2/CO) = 0.60	ER(SO_2/CO) = 0.70	ER(SO_2/CO) = 0.80
0.75	0.43	0.52	0.60	0.69
0.80	0.34	**0.41**	**0.48**	0.55
0.85	0.26	**0.31**	**0.36**	0.41
0.90	0.17	**0.21**	**0.24**	0.28
0.95	0.09	0.10	0.12	0.14

Ambient measurements of NO_2 and NOx started on 6th March when the smoke had already considerably abated. Between 6th and 25th March 2014, the maximum hourly CO concentration was 6 ppm. Measurements of NO_2/NOx and CO are not well correlated (r^2 of 0.58 and 0.34 respectively) which may be due to other sources of NO_2 and NOx other than the mine fire that contribute to the observed NO_2/NOx concentrations at Morwell South AMS. Additionally as for SO_2, the poor correlation between NO_2 and CO may also reflect the combustion conditions under which the two species are emitted. While NO_2 is an oxidised species dominantly emitted during flaming

combustion, CO is primarily emitted during smouldering combustion. As a result of this, no reliable EFs for NO_2/NOx could be derived from the ambient measurements at Morwell South AMS.

2.2.4 BENZENE, TOLUENE AND XYLENES

Figure 4 shows the expected linear relationship between VOC species and CO concentrations measured at Morwell South AMS between 26th February and 26th March 2014. Measurements started on 26th February and only a limited number of data points are available. The time series in Figure 5 shows that VOC concentrations decreased significantly in March and only two measurements were made during the more intense period of the fire.

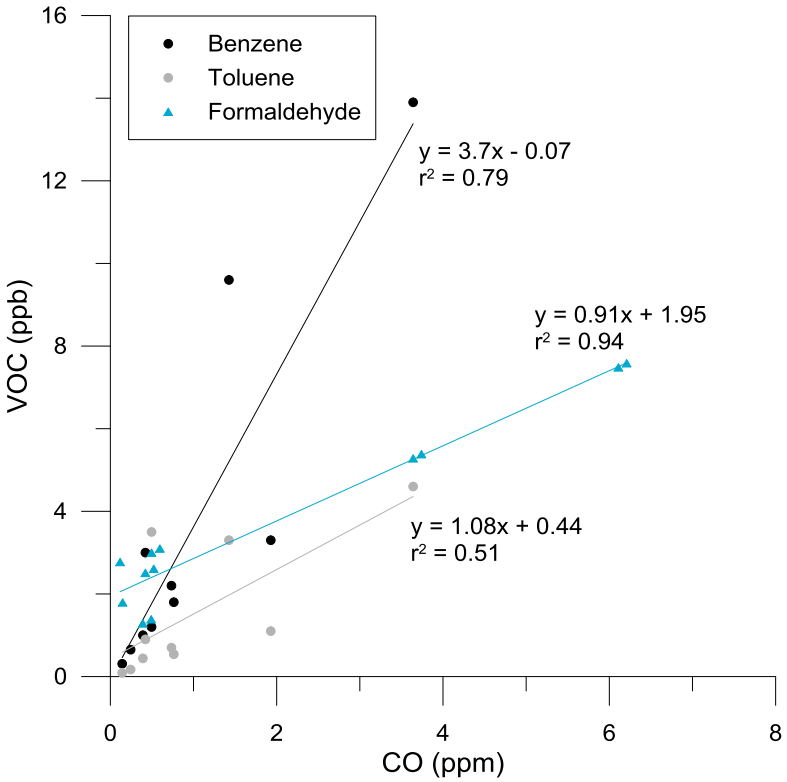

Figure 4 Relationship between selected VOCs and CO concentrations measured at Morwell South AMS.

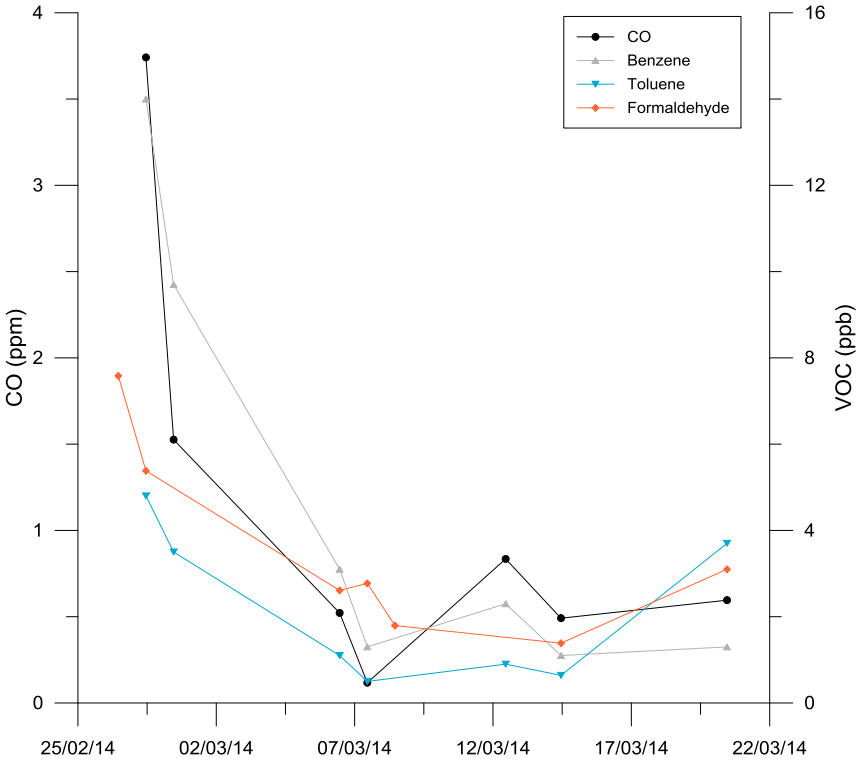

Figure 5 Time series of CO, benzene, toluene and formaldehyde concentrations measured at Morwell South AMS.

Table 5 presents the estimated range of emissions factors for benzene, toluene and formaldehyde using a range of MCE and ERs as determined (1) from the linear regression slope of the correlation between VOCs and CO and (2) from the two samples mostly impacted by smoke. The most likely EFs for the three VOCs (based on probable MCE and estimated ERs) are presented in bold. They range from 1.6 to 4.4 g kg^{-1} for benzene, from 0.5 to 1.8 g kg^{-1} for toluene and from 0.1 to 0.4 g kg^{-1} for formaldehyde. The median EFs are 2.7 g kg^{-1} ± 1.0 g kg^{-1} for benzene, 1.0 g kg^{-1} ± 0.4 g kg^{-1} for toluene and 0.3 g kg^{-1} ± 0.1 g kg^{-1} for formaldehyde.

Table 5 Estimated range of EFs for three VOCs (g kg^{-1} coal) determined by Eqs 3 and 4.

MCE	EF (Benzene) (g kg^{-1})		EF (Toluene) (g kg^{-1})		EF (Formaldehyde) (g kg^{-1})	
	ER = 3.7	ER = 5.3	ER= 1.1	ER = 1.8	ER= 0.9	ER = 1.3
0.75	3.9	5.5	1.4	2.2	0.4	0.5
0.80	**3.1**	**4.4**	**1.1**	**1.8**	**0.3**	**0.4**
0.85	**2.3**	**3.3**	**0.8**	**1.3**	**0.2**	**0.3**
0.90	**1.6**	**2.2**	**0.5**	**0.9**	**0.1**	**0.2**
0.95	0.8	1.1	0.3	0.4	0.1	0.1

2.2.5 PARTICLE COMPOSITION

Chemical analysis was conducted on eight PM_{10} and three size-fractionated filter samples collected during the Hazelwood mine fire. Chemical analysis included organic (OC) and elemental (EC) carbon, water-soluble ions, anhydrosugars and inorganics.

The fraction of OC, EC, sulfate (SO_4) and other components in collected PM_{10} and $PM_{2.5}$ samples is shown in Table 6.

Table 6 Chemical composition of $PM_{2.5}$ and PM_{10} particles.

Sample date	PM fraction	OC (%)	EC (%)	SO4 (%)	Other (%)
26/2-27/2	PM10	41	2	9	18
27/2-28/2		42	2	8	17
5/3-6/3		38	3	5	26
6/3-7/3		29	5	9	36
7/3-8/3		23	3	9	48
12/3-13/3		39	5	4	23
14/3-15/3		37	10	8	19
20/3-21/3		38	8	6	20
3/3-5/3	PM10	34	6	5	30
7/3-11/3		25	3	5	49
14/3-18/3		29	7	7	36
3/3-5/3	PM2.5	61	7	9	0
7/3-11/3		39	3	6	10
14/3-18/3		47	7	10	0

Based on an EF for $PM_{2.5}$ of 12 g kg^{-1}, the averaged EFs for OC, EC and SO_4 are 5.7 g kg^{-1} ± 1.4 g kg^{-1}, 0.8 g kg^{-1} ± 0.3 g kg^{-1} and 1.04 g kg^{-1} ± 0.25 g kg^{-1}, respectively.

Table 7 summarises the estimated EFs for relevant species used in the model in comparison to literature data.

Table 7 Estimated EFs of selected species in comparison to literature data.

Species	Hazelwood mine fire	Savanna[1]	Temperate forest[1]	Extratropical forest[1]	Peatland[1]	Charcoal burning[1]	Duff/organic soil[2]	Fire pit Anthracite[3]	Fire pit Bituminous[3]	Residential Anthracite[4]	Residential Bituminite[4]
CO	226	63	89	122	182	189	244	93	74		
SO2	0.34	0.48					1.76				
NOx	NA	3.9	2.51	1.12	0.80	1.41	-	1.1	2.6		
NH3	NM	0.52	0.78	2.46	10.8	0.79	2.67				
Benzene	2.7	0.20		1.11	2.46						
Toluene	1.0	0.08		0.48	1.21						
Xylenes	<DL	0.014		0.18							
Formaldehyde	0.3	0.73	2.27	1.92	1.69	0.60					
Acetaldehyde	NM	0.57			2.81						
Ethane	NM	0.66	1.12	1.70		0.41					
Ethanol	NM			0.055							
Methanol	NM	1.18	1.93	2.70	5.36	1.01					
$PM_{2.5}$	12	7.17	12.7	15.0			20.6	2.9	11.2	1.05	7.37
OC	5.7	2.62		8.6-9.7	6.23	1.3				0.47	2.98
EC	0.8	0.37		0.56	0.20	1.0				0.028	2.75
SO_4	1.04	0.018									

[1] Akagi et al. (2011); [2] Urbanski (2014); [3] Tian et al. (2008) ; [4] Zhang et al. (2008). NA= not available, NM=not measured, DL = detection limit

2.3 Amount of coal burned

The total amount of coal burned has been estimated by CSIRO using a bottom–up approach, involving the calculation of burn area, depth and density of the Hazelwood coal. For a fuel bed of substantial depth of which only the surface layer burns (e.g. an open-cut coal mine or peat bed), the commonly applied method is:

$$M_c = d.A.BD \quad (5)$$

Where Mc is the mass (g) of coal contained in an area *A* (m^2) and depth *d* (m) consumed over the duration of the fire and *BD* is the bulk density of the coal (g m^{-3}).

A set of images showing the area of active fire within the Hazelwood mine were obtained from the Country Fire Authority (CFA). These consisted of manually-drawn fire boundaries for the initial days of the fire, as well as aerial infrared firescan imagery at approximately daily intervals for the remainder of the fire. All images had a timestamp indicating their time and date of capture. Images were georegistered to local coordinates, and areas of active fire were digitized and stored in a GIS database along with their timestamp. The total area burnt (1.793×10^6 m^2) was determined from the infrared line-scan imagery provided by the CFA. For hourly fire activity, a raster cube was created at 100m spatial resolution covering the extent of the mine, with a time axis covering the entirety of February and March 2014 at hourly intervals, as the basis for the emissions grid. For time steps for which fire imagery was available, raster cells were attributed with the proportion of the cell containing active fire in that time step. Linear interpolation was then used to fill in the proportions of each spatial cell containing fire between times when imagery was available. A further weighting based on McArthur Forest Fire Danger Index (FFDI) (Mark 5) (Noble et al., 1980) was applied to cells between periods when imagery was available. Between each pair of available image times, FFDI values for the period of missing values were normalized to a mean value of 1, then applied as a multiplying factor to the interpolated fire area proportions. The Air Pollution Model (TAPM) generated hourly wind speed, temperature and relative humidity were used in the calculation of the fire danger index (see section 3.1).

In the absence of data on burn depth from the Hazelwood mine fire, the depth was estimated based on literature data from boreal peat fires which ranged from 0.01-0.3 m with an average peat burn depth estimated at less than 0.1 m. (Poulter et al., 2006; Van der Werf et al., 2006; Benscoter et al., 2011). The bulk density for Morwell brown coal of 1.115 g cm^{-3} was derived from Woskoboenko et al. (1991).

Using Equation 5, the total mass of coal burnt was estimated at approximately 140 kilo tonnes.

The rate of coal combustion was calculated by taking the total mass of coal burnt, as calculated above, and dividing it by the total area of coal burning throughout the fire from the raster cube integrated on an hourly time step. This emission rate was used to generate point-source emission inputs for two CSIRO modelling frameworks; near-field modelling and regional modelling. Emission factors are applied to the emission rates for the regional modelling to enable a full chemical breakdown of species to be represented.

3 Near-field modelling

In this Section, high-resolution modelling of $PM_{2.5}$ and CO concentrations due to the Hazelwood fire was conducted around Morwell during February–March 2014. For this purpose, CSIRO's The Air Pollution Model (TAPM v4.0.5) was used, which is an operational, three-dimensional, coupled prognostic meteorological and pollutant dispersion model (Hurley et al., 2005; Hurley, 2008; http://www.csiro.au/en/Research/OandA/Areas/Assessing-our-climate/Air-pollution/TAPM). TAPM has previously been applied to a variety of local- to regional-scale dispersion problems, and some examples of these include the studies by Luhar and Hurley (2003, 2012), Luhar et al. (2006, 2008), Zawar-Reza and Sturman (2008) and Bandeira et al. (2011).

TAPM uses input databases of terrain height, land use, leaf area index, soil type, sea-surface temperature, and synoptic meteorological analyses. The model can be used in one-way nestable mode to improve efficiency and resolution. The input synoptic data are specified for the horizontal wind components, temperature and moisture and given at 6-hourly intervals. The meteorological component of TAPM predicts the local-scale flow (e.g. terrain induced flows) against a background of larger-scale meteorology provided by the input synoptic analyses. Vegetative canopy, soil, and urban schemes are used at the surface. Measurements of wind speed and wind direction can optionally be assimilated into the model equations. The air pollution component uses the predicted meteorology and turbulence from the meteorological component, and consists of an Eulerian grid-based set of prognostic equations for pollutant concentration. An optional Lagrangian particle-puff mode for localised stack sources can be selected within the inner-most nest.

3.1 Meteorological modelling

3.1.1 MODEL SETUP

Atmospheric dispersion is governed by the meteorology of the area being considered and, therefore, it is crucial that TAPM is configured and tested such that it closely represents the local meteorology. For meteorological configuration, the model was setup with four nested grid domains at 30, 10, 3, 1 km resolution for meteorology (25 × 25 grid points), all centred on (146°28′ E, 38°12.5′ S), which is equivalent to 453.307 km east and 5770.935 km north in the MGA (Map Grid of Australia, Zone 55) coordinate system. The lowest ten of the 25 vertical levels were 10, 25, 50, 100, 150, 200, 250, 300, 400 and 500 m, with the highest model level at 8000 m. The innermost domain covers an area of 25 km × 25 km and included the Morwell South, Morwell East and Traralgon locations for which meteorological observations were available. The model was run for two months covering February–March 2014. The hourly-averaged model meteorological predictions on the innermost grid domain were extracted at the grid point nearest to each of the three monitoring stations for comparison with the data.

A number of model runs were performed with the aim of achieving an optimised setup for its ability to describe the observed meteorology. The use of TAPM's default input databases provided a reasonable comparison with the meteorological data. However, it was found that the use of the European Centre for Medium-Range Weather Forecasts' ERA-Interim synoptic reanalyses given at a horizontal resolution of 0.75° × 0.75° resulted in a better performance by TAPM than when the default US National Center for Environmental Prediction's synoptic reanalyses given at 2.5° × 2.5° resolution were used.

Similarly, the use of an Australian land-cover database ("vege.aus" file) developed by then CSIRO Wildlife and Ecology at an approximate grid spacing of 5 km showed a better representation of the actual land cover within the model domains under study than TAPM's default global land-cover data from the US Geological Survey given at approximately 1-km grid spacing. However, unlike the default land-cover

database, the CSIRO database did not categorise the towns of Morwell and Traralgon as urban, contrary to their being so. Therefore, the TAPM land-cover file was edited such that these towns were represented as urban.

3.1.2 COMPARISON WITH DATA

The above TAPM setup provided the best comparison with the winds and temperature data at Morwell and Traralgon. Hourly meteorological data at 10 m above ground level from two EPA Victoria monitoring stations in the area were available: Morwell East (146.424°E, 38.229°S), starting on 13th February 1300 h (sample size = 1115); and Morwell South (146.393°E, 38.242°S), starting on 21st February 1200 h (sample size = 925). These data were also available from an EPA Victoria station at Traralgon (146.527°E, 38.195°S) from 8th February 2400 h (sample size = 1225). These times are in AEST and correspond to the end of hourly averaging period. The same time convention is used in TAPM modelling

Figure 6a shows scatter plot of the model predictions vs. observed data for wind speed at Morwell East. This comparison suggests a good performance by the model, both in magnitude and correlation, with a correlation coefficient value of 0.77. The model performance for Morwell South and Traralgon was similar (plots not shown) with correlation coefficient values of 0.76 and 0.80, respectively. The temperature was predicted very well at all three sites (plots not shown) with a correlation coefficient value between 0.92–0.94.

Figure 6b presents the normalised frequency of occurrence of the observed and modelled wind direction at Morwell East (the plots, not shown, are qualitatively similar for Morwell South and Traralgon). To make this plot, the values of wind direction were binned and the number of values in a particular bin were normalised by the total number of values to obtain the normalised frequency. The data point is plotted for the upper value of the bin range, e.g. 15 deg. for 0–15 deg. Figure 6b shows that the model is able to reproduce the broad features of the observed wind-direction frequency distribution, with peak frequencies occurring in the NE-SE and SW-NW sectors. However, it is clear that there are significant shifts between the modelled and observed frequencies within these broad sectors. For near-source concentration predictions at a given time and location, such differences in wind direction can adversely impact model-data comparison because in such cases the modelled direction of plume transport can deviate significantly from that observed. If the concentration predictions are done for population exposure assessment in which spatial distribution of population is considered, it is particularly important that the model predicts the direction of the plume transport consistent with the observed wind direction.

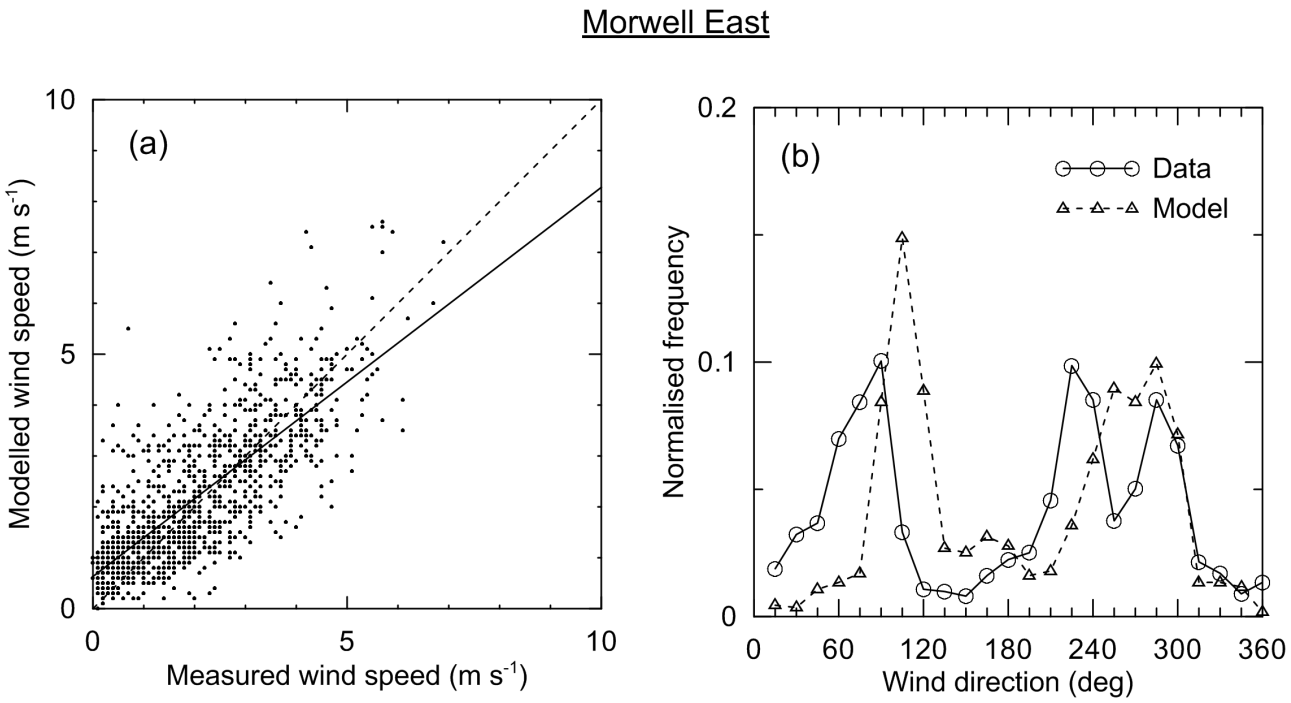

Figure 6: (a) Scatter plot of model predictions vs. observed data for wind speed, and (b) the normalised frequency of occurrence of the observed and modelled wind direction at Morwell East.

One way to reduce inaccuracy in the predicted winds and hence to improve the near-field concentration simulation is to apply a procedure known as "wind data assimilation" which adjusts the wind speed and wind direction in the model to those observed in the atmosphere. This method is useful where there are wind observations and there is no extreme variations in topography. In TAPM, wind observations can optionally be assimilated into the momentum equations as nudging terms that push the model gently towards observed values. The nudging term should be large enough to be noticed by the model, but not so large that it dominates over other terms in the equation. Generally, winds predicted with assimilation would be very close to the assimilated observations, but may not be exactly the same. The hourly-averaged wind speed and direction observations from Morwell East and Traralgon were assimilated into TAPM. Because Morwell East started operating on 13th February whereas Traralgon on 8th February, and given the fact that there is a good correlation between the Morwell East and Traralgon wind data, the Morwell East wind data was gap filled by the Traralgon data for the duration 8th – 13th February. The resulting comparison shown in Figure 7a and b for Morwell East suggests that the modelled wind deviations from the observations have been reduced considerably compared to Figure 6. Figure 7 also presents comparison plots (c–f) for Morwell South and Traralgon, which too are an improvement over the model predictions without wind data assimilation for these sites.

In the following, the above meteorological configuration of TAPM was used with wind data assimilation for plume dispersion predictions for $PM_{2.5}$ and CO around Morwell. (Plume dispersion modelling without wind data assimilation was also carried out, but assimilation led to somewhat better model evaluation with the concentration data around Morwell.)

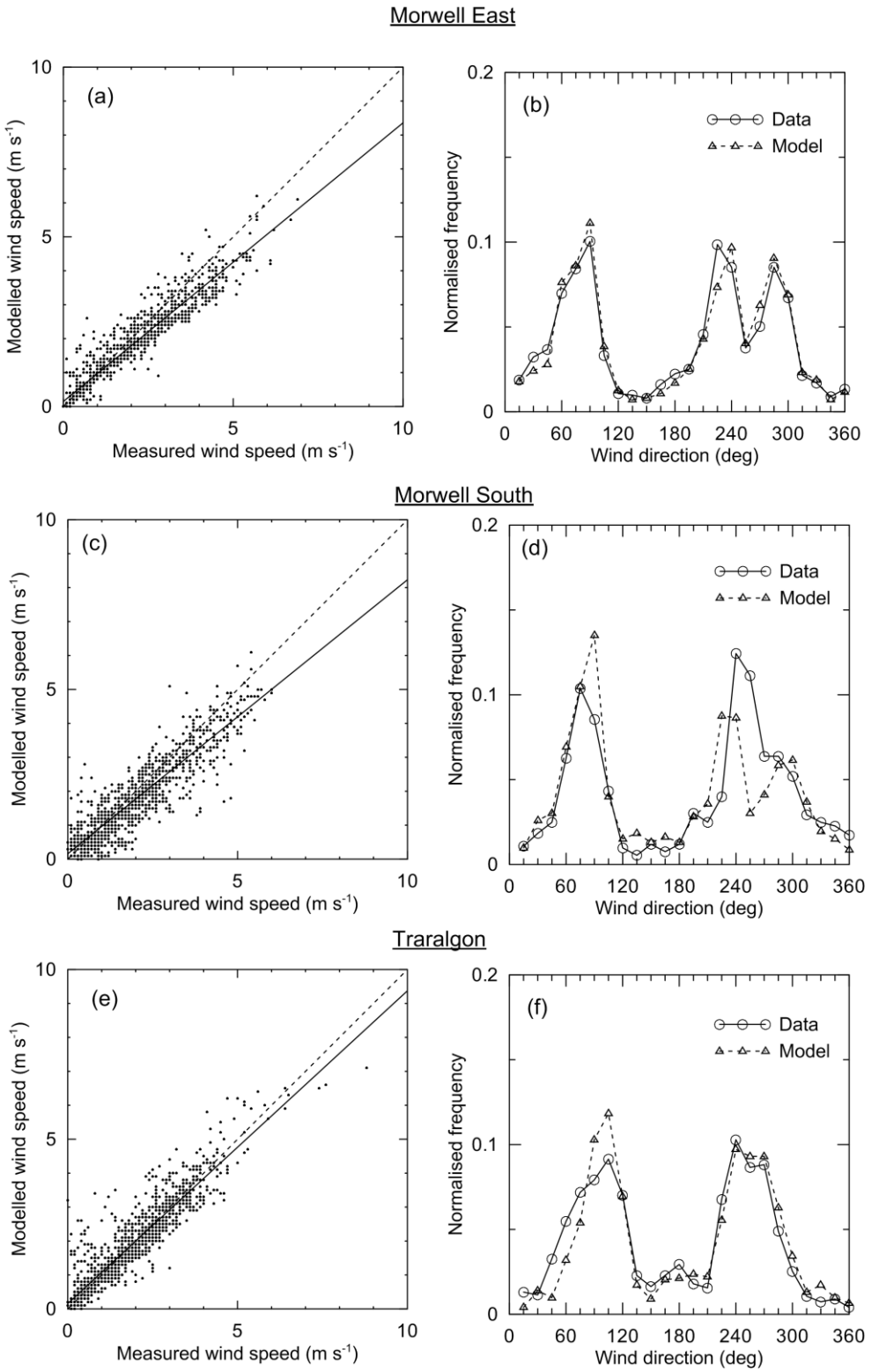

Figure 7: (a) Scatter plot of model predictions vs. observed data for wind speed, and (b) the normalised frequency of occurrence of the observed and modelled wind direction at Morwell East; (c) and (d) those at Morwell South; and (e) and (f) those at Traralgon. Wind data assimilation used in TAPM.

3.2 Plume dispersion and concentration modelling

3.2.1 MODEL SETUP

The following grid setting was used for high resolution modelling of plume dispersion. As before, TAPM was run with four nested domains of 25 × 25 horizontal grid points at 30-km, 10-km, 3-km and 1-km spacing for meteorology with wind data assimilation. For dispersion, 101 × 101 horizontal grid points at 3-km, 1-km, 300-m and 100-m spacing were selected. 25 vertical levels were used as before. All domains were centred on (146°24.5′ E, 38°15′ S), which is equivalent to 448.230 km east and 5766.281 km north in the MGA (Zone 55) coordinate system. The innermost dispersion domain covers an area of 10 km × 10 km and includes Morwell South and Morwell East (see Figure 8). The next dispersion domain of 300-m spacing covers an area of 30 km × 30 km and includes Traralgon.

The total spatial extent of the coal fire was determined based on fire maps. It was a rectangular area which was divided into 50 × 35 grid points with a spacing of 100 m, and each of these grid points was treated as a point source. Hence, there was a total of 1750 point sources, each 100-m apart (see Figure 8). At a given time, some of these point sources would have finite emissions and some would have zero emissions depending on the fire activity at the time. The hourly rate of mass of coal burnt for each point source was determined as described in Section 2.3. The median emission factor values of 226 g CO and 12 g $PM_{2.5}$ per kg of coal burnt estimated in Section 2.2 were then applied to determine the hourly emissions of these species for each source. For the near-field modelling, both CO and $PM_{2.5}$ were treated as passive tracers. TAPM's default Eulerian option for pollutant concentration was used for each source.

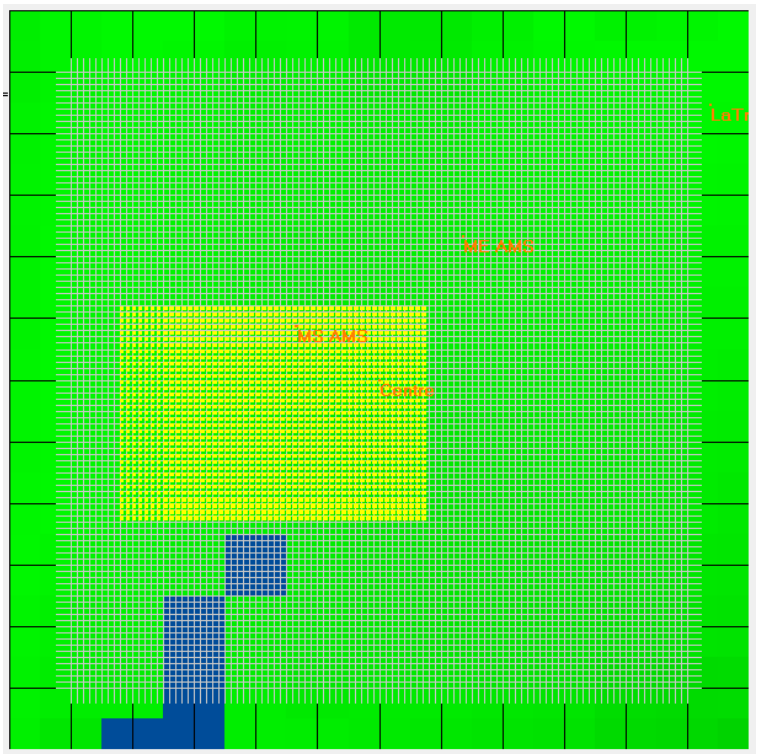

Figure 8: TAPM's innermost dispersion domain (grey region) and the selected domain of the mine fire which encompasses emission sources (yellow region). The innermost dispersion domain covers an area of 10 km × 10 km with a resolution of 100 m × 100 m and 101 × 101 grid points, and includes Morwell South (MS) and Morwell East (ME). The emission source area consists of 50 × 35 grid points, each representing a point source 100 m apart (a total of 1750 point sources). At a given time only some of these sources are emitting depending on the fire activity. Centre is the centre point of the dispersion domain. The black lines are 1 km apart and represent the innermost meteorological resolution. The blue area is water.

3.2.2 PLUME RISE FORMULATION

Hot smoke plumes released from localised sources into the atmosphere drift upward owing to their positive buoyancy. Inclusion of plume rise in dispersion models is important as it influences both plume dispersion and height of plume travel, with consequences for ground-level concentrations. Photos of Hazelwood smoke plumes suggest a varied level of plume rise, from almost no plume rise to heights of the order of 100 metres. Typically, a plume rises as it travels downwind and at some distance from the source it attains a final (or equilibrium) height as a result of ambient stability and/or turbulence. Turbulence generated by plume's buoyancy also contributes to the spread of plume around its centreline. In most models, including TAPM, the final plume rise is treated as a virtual source height and the buoyancy-generated plume spread is added to that caused by ambient turbulence. However, TAPM's plume rise algorithm is designed for industrial stack plumes, and requires input values such as stack radius, stack exit velocity and stack exit temperature. Thus, this algorithm is not appropriate for free burning fires such as that at Hazelwood.

Zonato et al. (1993) derived the following formula for final plume rise (Δh) for free burning fires:

$$\Delta h = 4.2 \frac{[(1-E)Q_H]^{0.26} L^{0.63}}{u^{0.5}}, \qquad (6)$$

where E is the fraction of the heat released in the environment as thermal radiation (= 0.3), Q_H is the total heat rate (kcal s^{-1}), L is the diameter of the fire (m), and u is the wind speed (m s^{-1}).

In our modelling, the source resolution is 100 m × 100 m, which is equivalent to a circular source area of diameter L = 113 m. The average energy content of Victorian lignite brown coal is 8.4 MJ kg^{-1} (= 2007 kcal kg^{-1}). This value was multiplied by the amount of coal burnt per hour (Q_c) to obtain Q_H for each source.

The above formula assumes that the entire source area of diameter L is burning. This, however, is not the case in the present situation where only a small part of the source area of 100 m × 100 m may be burning during a given hour. It is assumed that L is proportional to the hourly coal burning rate (Q_c) for a source normalised by the maximum value of the hourly coal burning rate for any source for the entire fire period (Q_{max}). It is further assumed that when $Q_c = Q_{max}$, L is 90% of that when the entire source area of diameter L is burning. Hence the new expression for L is:

$$L_{new} = 0.9\, L \frac{Q_c}{Q_{\max}}, \tag{7}$$

which is substituted in Eq. (6).

The above plume rise formula was used in TAPM for each point source, and was initialised using the modelled wind speed (u) at a height of 50 m and then iterated for wind speed at the plume rise height.

The plume radius (r_p) due to buoyancy generated turbulence is determined as per the original TAPM scheme:

$$r_p = \beta.\Delta h, \tag{8}$$

which is combined with the plume spread due to ambient turbulence, where the entrainment constant $\beta = 2/3$.

The TAPM dispersion configuration was run for the period February–March 2014. The hourly-averaged modelled concentration predictions resulting from all coal fire sources were extracted at the grid point nearest to each of the monitoring stations for comparison with the $PM_{2.5}$ and CO data. Hourly plume rise values were also extracted for all non-zero emission coal fire sources. Hourly background concentrations simulated using a regional run of CCAM-CTM without the coal fire emissions (see Section 4.1) were added to the TAPM simulated concentrations.

Figure 9 presents a histogram (in terms of normalised frequency) of hourly plume rise values for the coal fire sources simulated by TAPM. About 60% of the time plume rise lies within 0–20 m, 18% of the time within 20–40 m, and the frequency steadily decreases for higher values of plume rise. There are some instances of plume rise within the height range of 180–200 m.

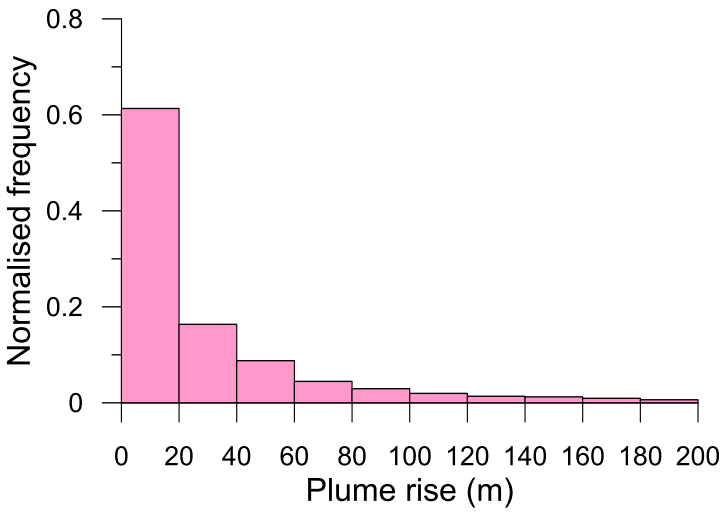

Figure 9: Histogram (normalised frequency) of the modelled hourly plume rise values (based on 100231 data points).

3.2.3 CONCENTRATION COMPARISON

In this section the modelled concentrations of CO and $PM_{2.5}$ are compared with those measured at Morwell South, Morwell East and Traralgon. These measurement sites are almost aligned along a straight line relative to the mine source.

Figure 10 presents time series of the hourly-averaged observed and modelled concentrations of $PM_{2.5}$ and CO at Morwell South. The concentration measurements were only available from 20th February. In Figure 10a, concentrations of $PM_{2.5}$ as high as 3700 μg m^{-3} are predicted by the model during 9–10 February, followed by virtually no concentrations as the wind direction changes and transports the plume away from the monitoring station. The modelled concentration starts increasing again from 13th February. The model predicts very low $PM_{2.5}$ concentrations from 8th March onwards when there is virtually no coal burning (as inferred from the fire maps used to calculate the emissions). For the period 20th February – 8th March, the model simulates the magnitudes of the observed concentration fairly well.

In Figure 10b for CO, the model predicts concentrations as high as almost 60 ppm in the early phase of the fire. As in the case of $PM_{2.5}$, the model describes the measurements reasonably well until 7th March, after which the emissions used are very low resulting in very low modelled CO concentrations; however, the observed time series shows significant concentration peaks on some days.

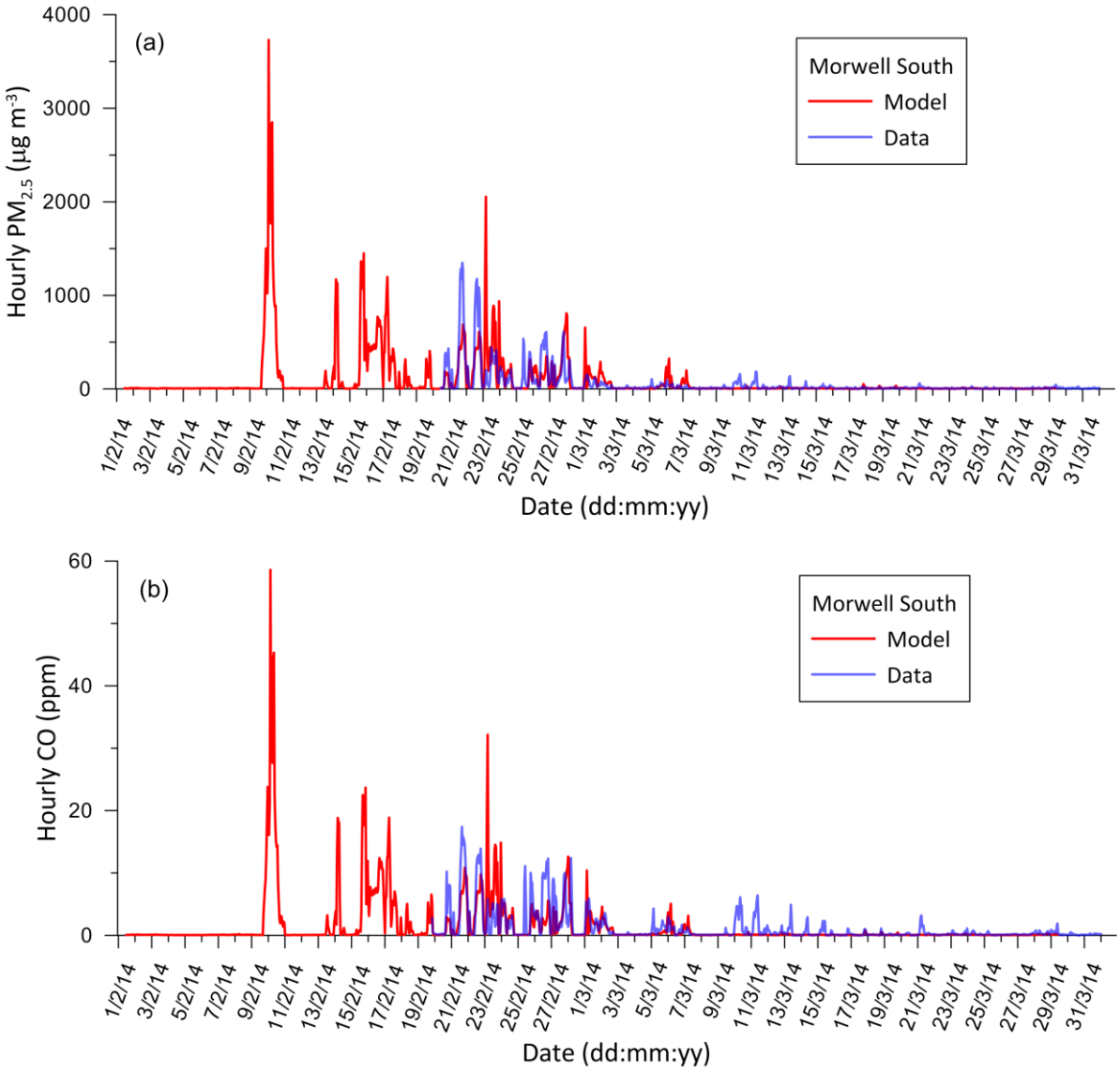

Figure 10: Time series of the hourly-averaged observed and modelled concentrations of (a) PM2.5 and (b) CO at Morwell South.

Figure 11 is the same as Figure 10 but for Morwell East. This site is about 3 km further downwind from the mine source. Both the observed and modelled concentrations are lower than those for Morwell South. Again, the highest concentrations are predicted during the early phase of the fire, and the model is able to capture the magnitudes of the observed concentration time series for both $PM_{2.5}$ and CO.

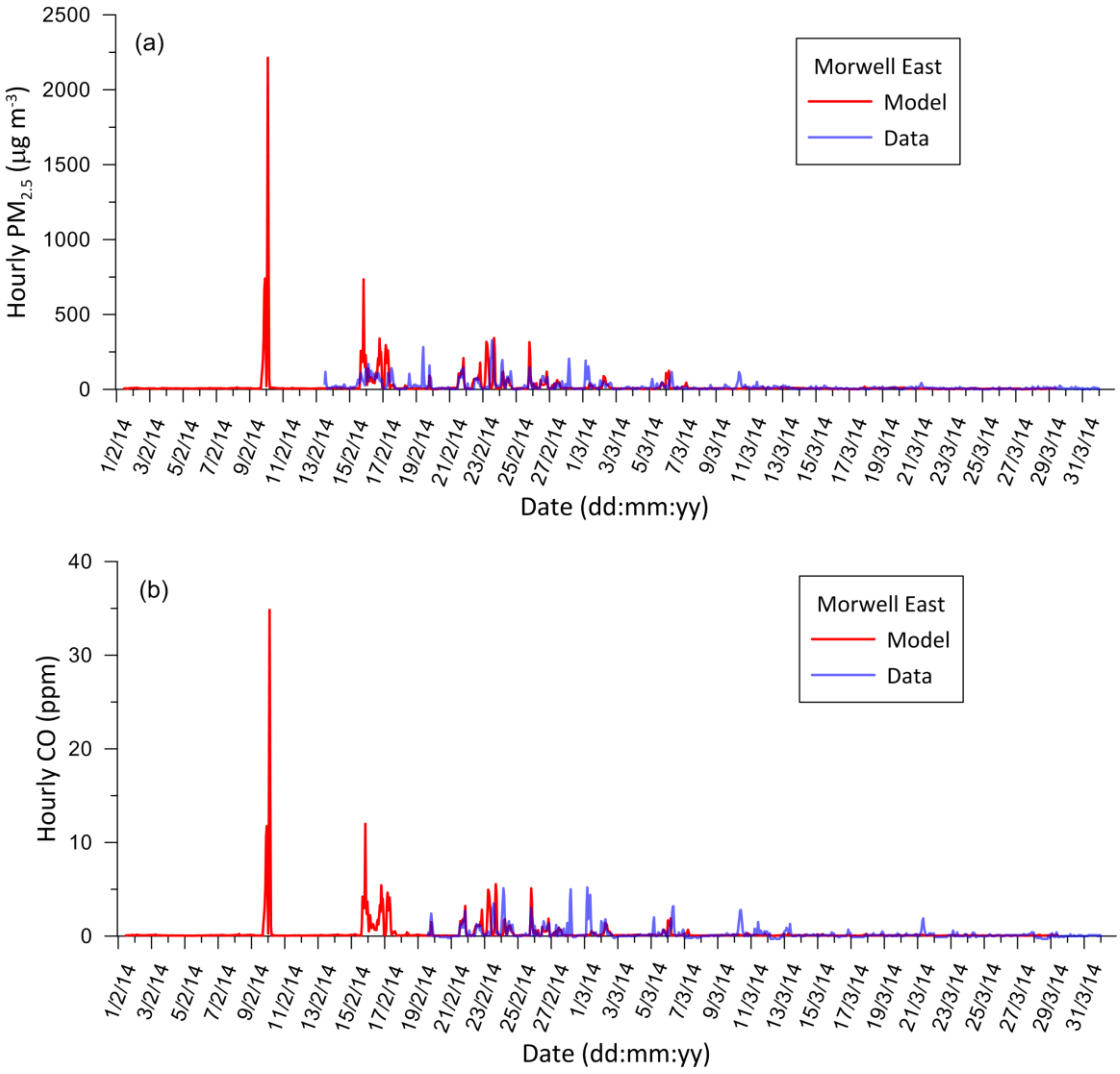

Figure 11: Time series of the hourly-averaged observed and modelled concentrations of (a) PM2.5 and (b) CO at Morwell East.

Figure 12 is for Traralgon, which is about 15 km north-east from the mine source. Both the modelled and observed concentration peaks of $PM_{2.5}$ and CO at this site are much lower than those for Morwell South and Morwell East because of the greater distance from the source. There is some observed variability in CO following 8 March which is not captured well by the model.

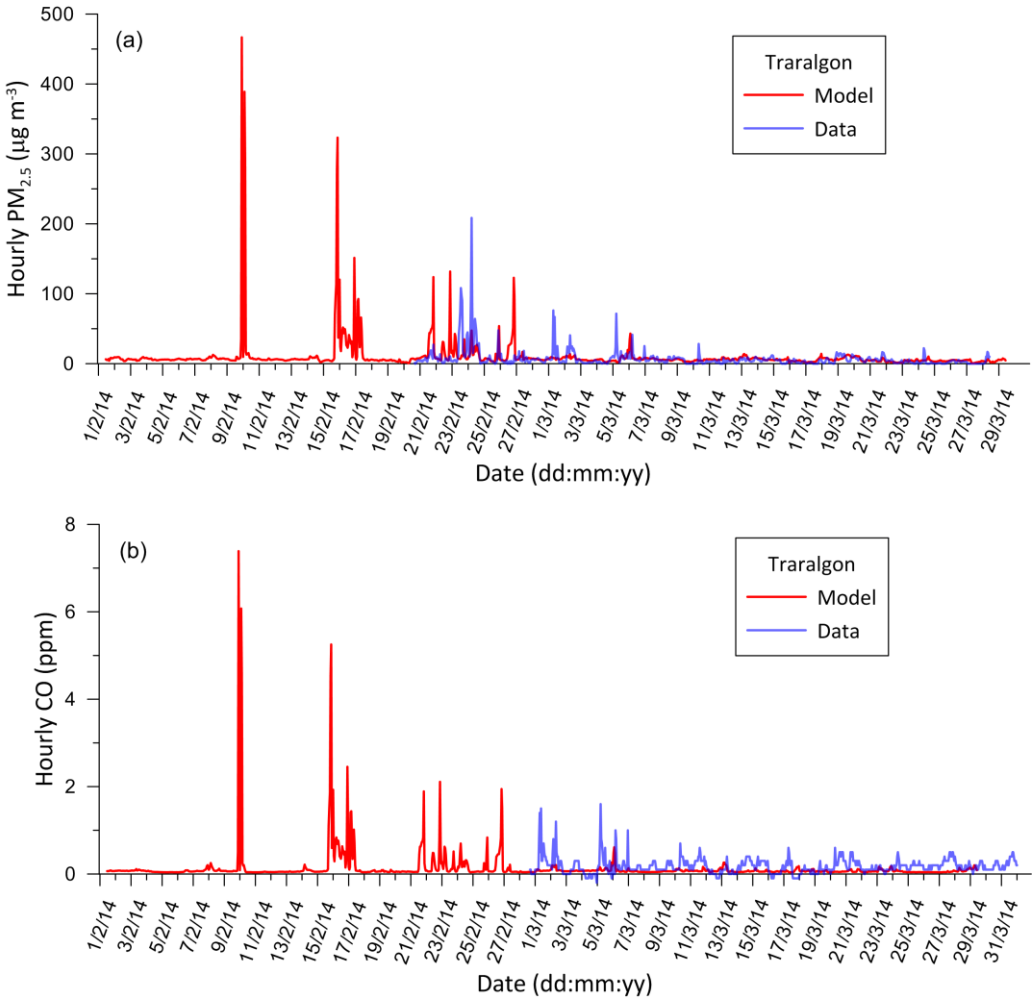

Figure 12: Time series of the hourly-averaged observed and modelled concentrations of (a) PM2.5 and (b) CO at Traralgon.

Scatter plots of the hourly-averaged modelled vs. measured concentrations are shown in Figure 13. There is considerable scatter in these plots, which is typical of air quality model evaluation studies involving hourly concentrations paired in both space and time. For Morwell South, the correlation coefficient (*r*) is 0.57 for both $PM_{2.5}$ and CO. For Morwell East, *r* is 0.37 for $PM_{2.5}$ and 0.32 for CO. At this site, there are some observed high concentrations which are not predicted by the model. Similarly, on occasions the model predicts high concentrations but they are not present in the measurements. At Traralgon there is a mismatch as to when the high concentrations of $PM_{2.5}$ occur in the model and measurements, but the magnitudes of the modelled and measured high concentrations are similar. The model underestimates CO at Traralgon. The measurements of CO at this site are only available from 1st March onwards; there is very little emission from the coal fire for this period using the adopted emission methodology which results in the modelled concentrations being lower.

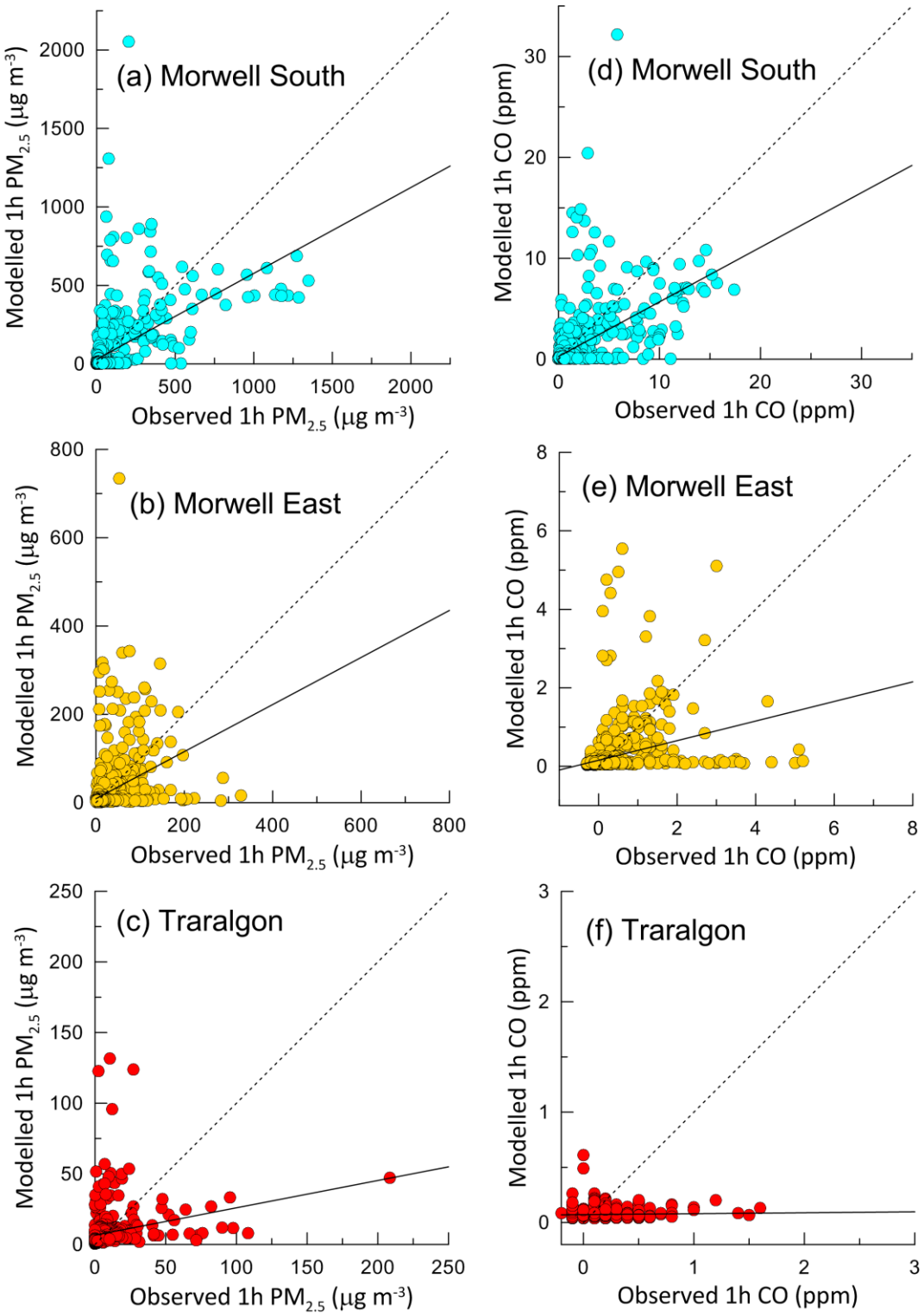

Figure 13: Scatter plots of the hourly-averaged modelled vs. measured concentrations for PM2.5 (left panels) and CO (right panels) for Morwell South, Morwell East and Traralgon.

Comparison of observed and modelled concentrations paired in both space and (hourly) time, as presented above, is a stringent test of an air dispersion model. On occasions TAPM does not predict the observed temporal maxima at the same time. A quantile-quantile (q-q) plot, in which sorted modelled concentrations are plotted against sorted observed values (i.e. unpaired in time) at a monitoring location, is often used in air quality model evaluation studies in order to examine any model bias over the full concentration distribution at that location. (Q-q plots for concentrations unpaired in both space and time are also commonly used.) The q-q plots in Figure 14 show that there is some underestimation of the observed concentration distributions at Morwell South; and overestimation of $PM_{2.5}$, and underestimation of CO for mid-range concentrations, at Morwell East. CO at Traralgon is underestimated as discussed above.

There could be various reason for the model-data differences such as uncertainty in the emissions methodology and emission factors, plume rise parameterisation, and the local wind flow not represented by the model at every scale. However, overall, as suggested by the q-q plots the model simulates the concentration distribution satisfactorily, barring CO at Traralgon.

In Australia, the air quality limits (or standards) for $PM_{2.5}$ particles and CO are 25 $\mu g\ m^{-3}$ as a 24-hour average and 9 ppm as an 8 hour average, respectively. The fine-scale modelling shows that, overall, residents of Morwell were exposed to the greatest number of breaches of the $PM_{2.5}$ limit, exceeding the limit on 23 days at Morwell South and 12 days at Morwell East locations out of a total 45 days the fire burned. There were 5 breaches of the $PM_{2.5}$ limit at Traralgon. The limit for CO was exceeded 7 times at Morwell South.

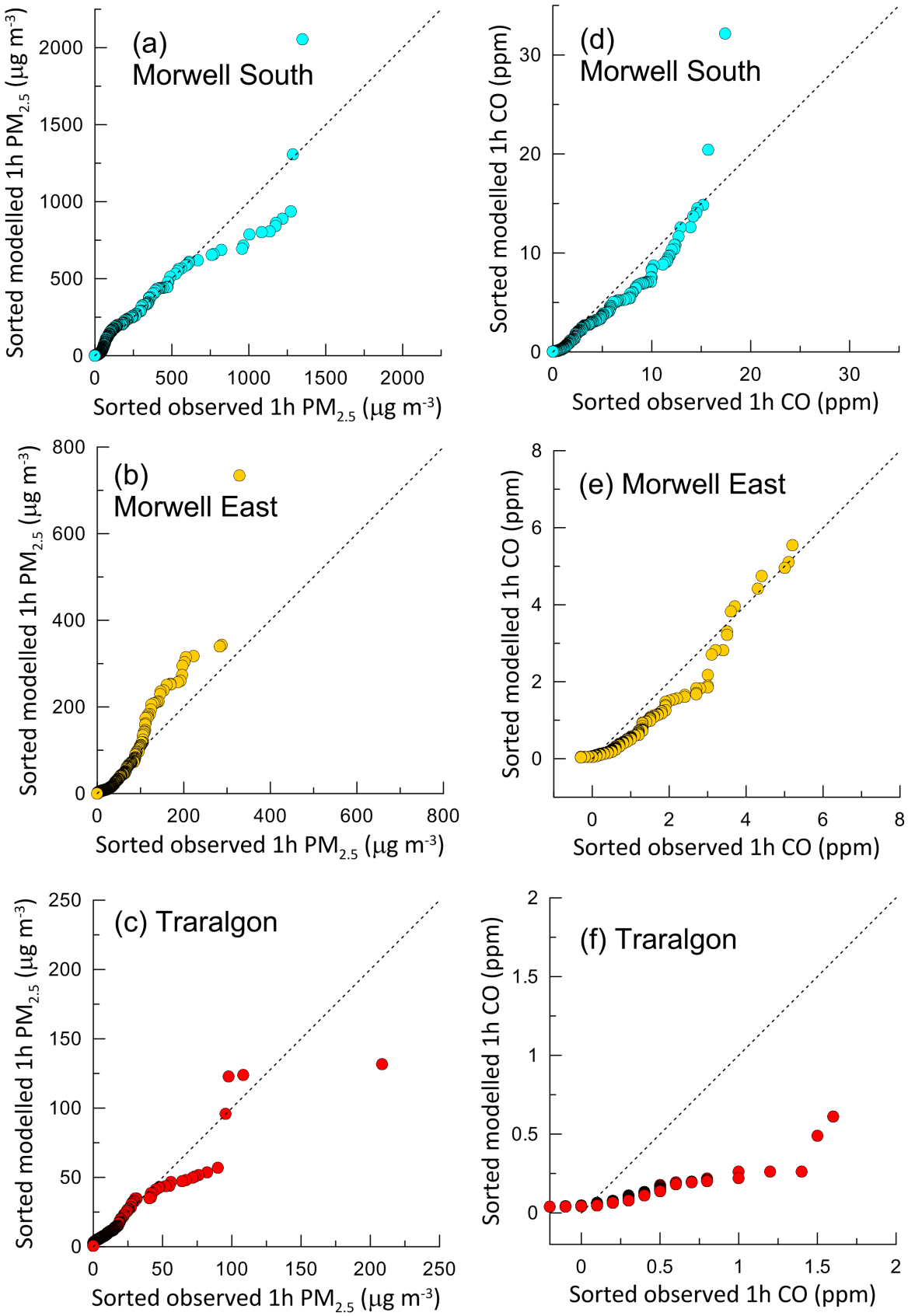

Figure 14: Quantile-quantile (q-q) plots of the sorted hourly-averaged modelled vs. sorted measured concentrations for PM2.5 (left panels) and CO (right panels) for Morwell South, Morwell East and Traralgon

4 Regional modelling

The CSIRO Chemical Transport Model (CTM) has been set up using the same nested grids described in Emmerson et al. (2015), from a resolution of 80 km at the Australia scale down to 1 km close to Morwell. The meteorology is provided to the CTM from the Conformal Cubic Atmospheric Model (CCAM) (McGregor and Dix, 2008).

Emissions for the model are taken from five different sources:

1) Anthropogenic emission inventory from the Victorian EPA (2006)
2) Sea salt, wind-blown dust and biogenic (vegetation based) volatile organic compound emissions are calculated within the CTM from wind speed and temperature profiles provided by CCAM
3) Australian wildfire emissions from the Global Fire Assimilation System (GFAS) (Kaiser et al., 2012).
4) Victorian wildfire emissions, estimated from fire scar data from the Department of Environment, Land, Water and Planning (DEWLP).
5) Estimated smoke emissions from the Hazelwood mine fire.

The CTM was run from February 1st 2014 to allow for at least one weeks' 'spin-up' time before the Hazelwood mine fire started. This allows the initial conditions within the model to settle down and reach equilibrium. The model was run through the mine fire period till March 28th 2014.

4.1 Background concentration modelling

CSIRO has undertaken regional background chemical transport modelling to estimate the concentrations of CO and $PM_{2.5}$ present in the impacted region in the absence of the Hazelwood mine fire. The modelling includes all the sources listed above except 5, and identifies periods when the regional background concentrations of CO and $PM_{2.5}$ are likely to make a significant contribution to exposure in the impacted regions. These background sources include the Victorian and Australian wildfire smoke. As pointed out in Section 3.2, this modelling also provides background concentrations to be added to the near-field concentrations predicted by TAPM. Doing background modelling is also useful if the air quality effects solely due to the mine fire are required: as chemical modelling is a highly non-linear process, it is not possible to run the mine fire emissions by themselves in the absence of other emissions at regional scale. Figure 15 shows the time series of the modelled background $PM_{2.5}$ against the observed $PM_{2.5}$. (The time stamp is in AEST). The influence of the Hazelwood mine fire on the observed $PM_{2.5}$ is very clear, with concentrations not matching the magnitude of the modelled time series until the later stages of March, particularly at the two Morwell sites. Predicted background $PM_{2.5}$ concentrations at Morwell South are 6 $\mu g\ m^{-3}$ on average, which is similar to predicted $PM_{2.5}$ concentrations at the other sites.

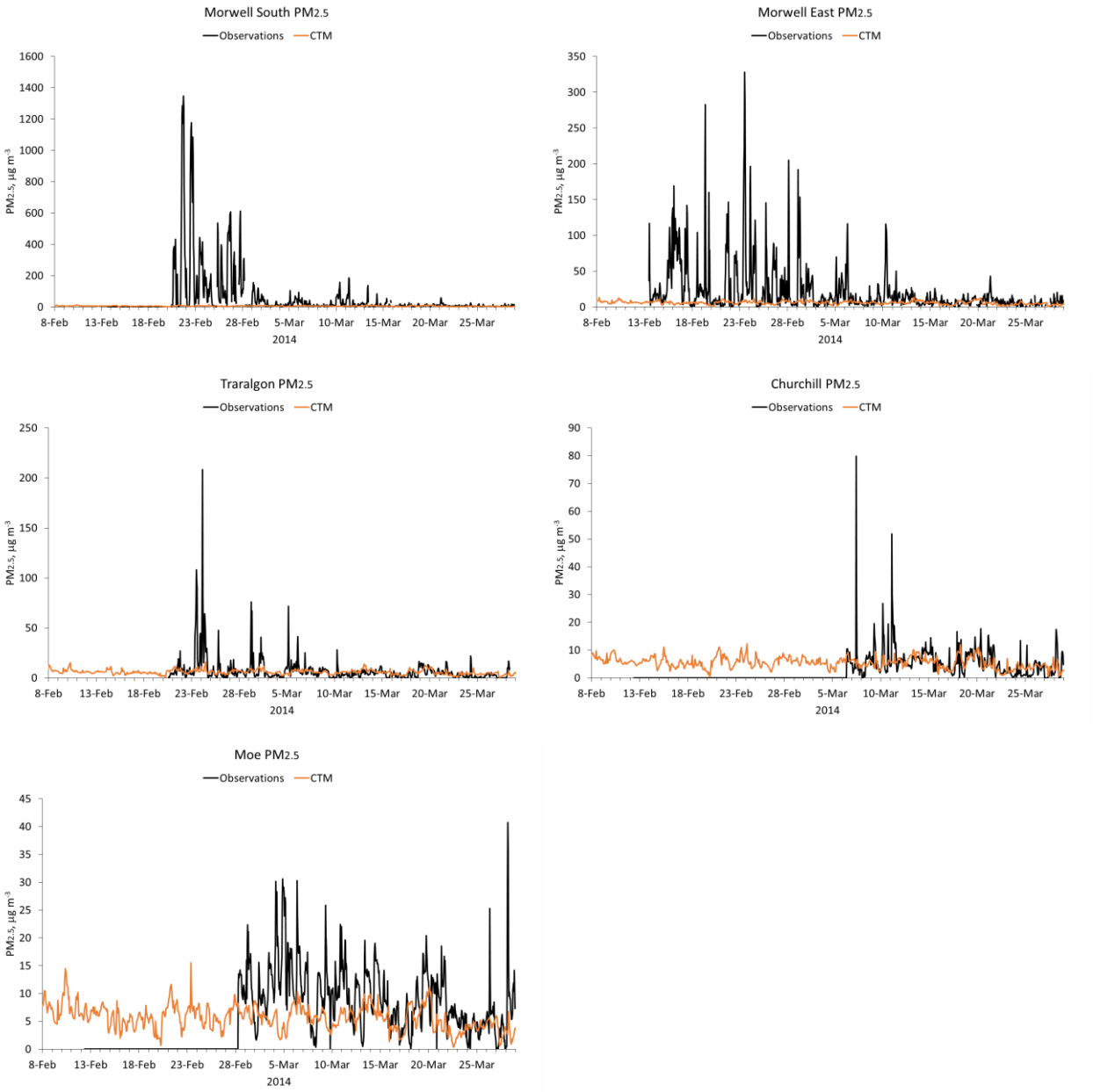

Figure 15 Time series of hourly observed $PM_{2.5}$ compared with predicted $PM_{2.5}$ from the background concentrations run. Note, y-axes are not the same in each plot.

Concentrations of observed $PM_{2.5}$ at Churchill and Moe reach background levels after 12th March. Figure 16 shows similar time series of observed and predicted background concentrations for CO. Note that CO is not monitored at Churchill and Moe. Background predicted concentrations of CO at the Morwell South site are 0.07 ppm, again similar to the predicted CO concentrations at the other sites.

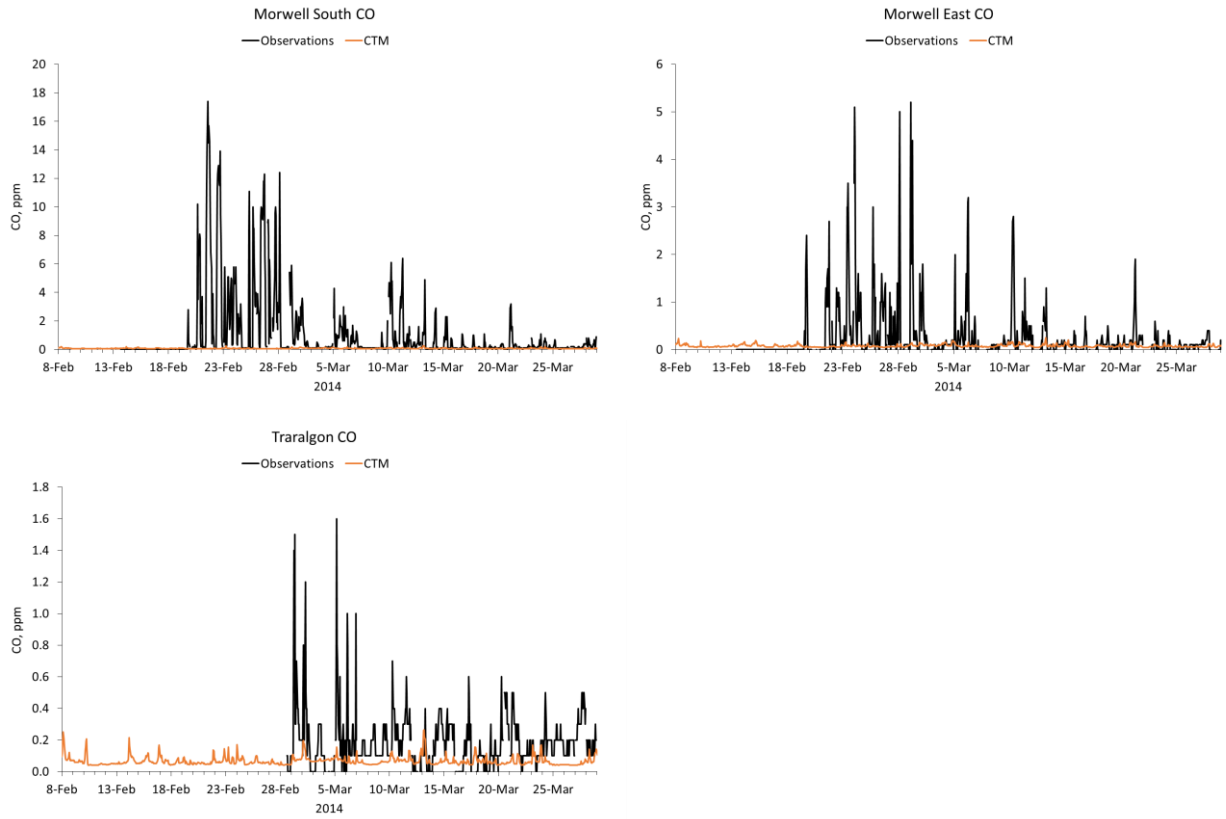

Figure 16 Time series of hourly observed CO compared with predicted CO from the background concentrations run. Note, y-axes are not the same in each plot.

From these results, it is expected that the smoke from the Hazelwood mine fire did not impact air quality in the nearby Latrobe Valley towns after March 12th. Figure 17 shows the spatial extent of the predicted $PM_{2.5}$ and CO concentrations in the Latrobe Valley. Background concentrations of $PM_{2.5}$ are highest over the sea and coastal regions due to sea salt aerosol. Concentrations of $PM_{2.5}$ are lowest at altitude over the hills. By contrast, background concentrations of CO are highest within the valley due partly to anthropogenic activity and partly to emissions from the four power stations in the region.

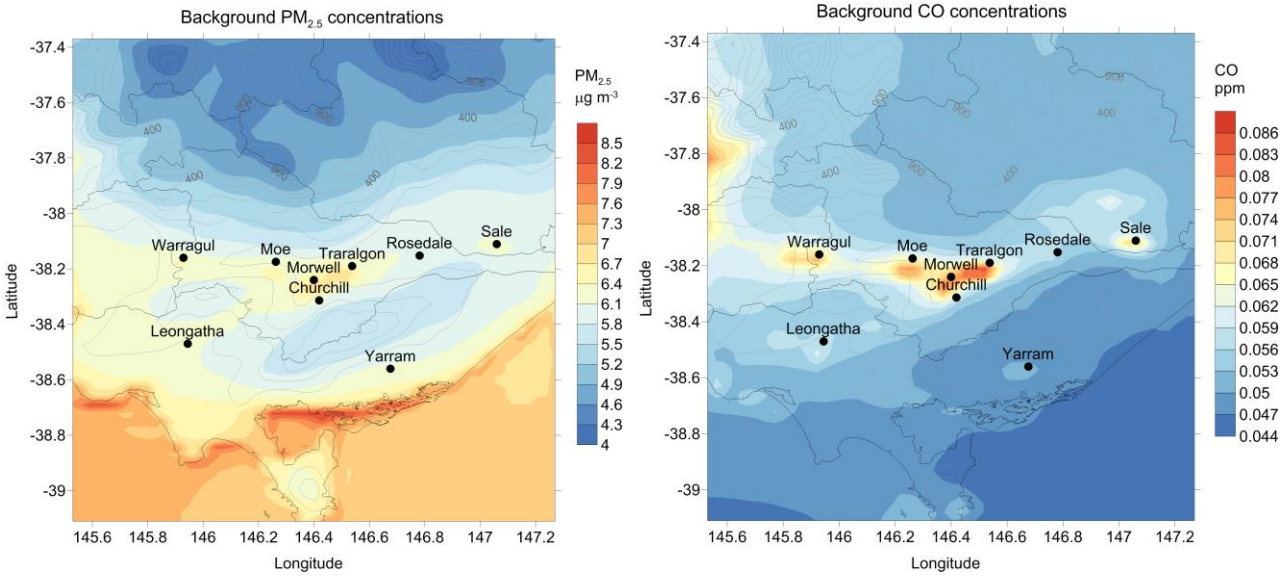

Figure 17 Maps to show predicted average background concentrations of $PM_{2.5}$ and CO in the Latrobe Valley across February and March 2014.

4.2 Inclusion of the Hazelwood mine fire

The near-field modelling predicted the degree of plume rise of the smoke emitted from the mine fire. This was used to inform the CTM on the initial height the mine fire smoke is emitted. Figure 18 shows the smoke plume reached 100 m to 200 m during the first 15 days of the mine fire, reducing to less than 50 m in the later phase of the fire. This demonstrates the effect of the intensity of fire on plume rise. There is a diurnal cycle to the smoke plume rise which mirrors the rise and fall of the atmospheric boundary layer during the day and night, respectively.

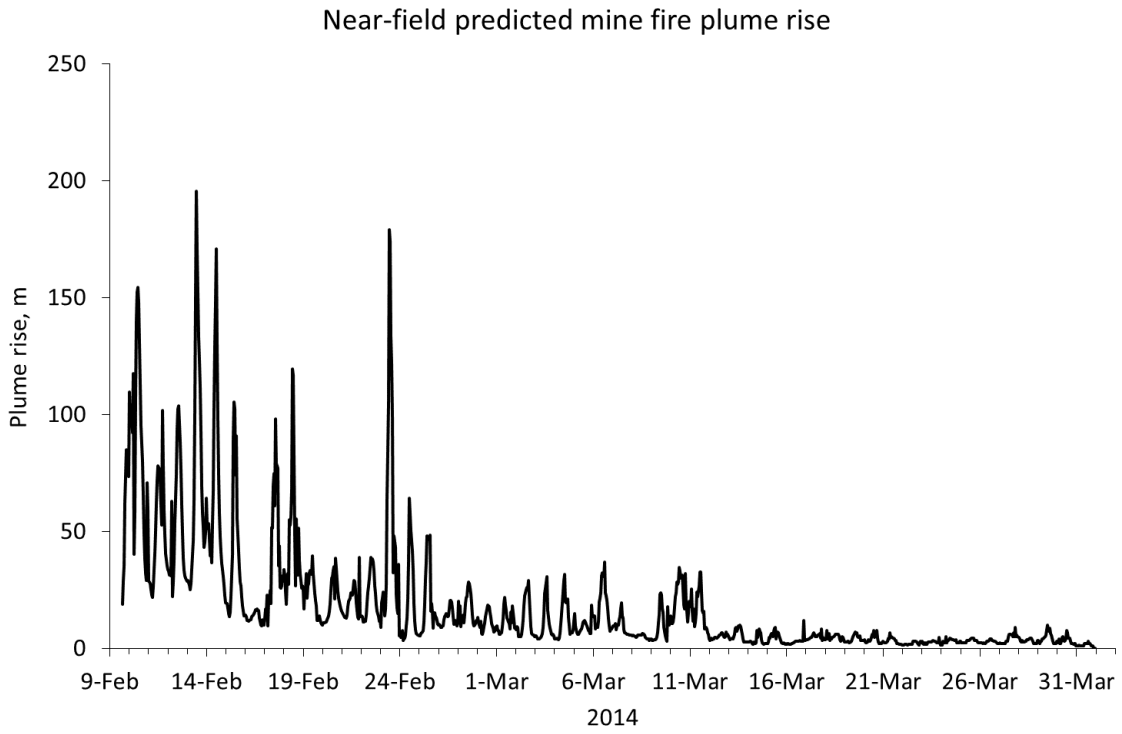

Figure 18 Near-field modelled, spatially-averaged plume rise values for the coal fire plume.

Figure 19 shows the results for $PM_{2.5}$ from the CTM using the estimated mine fire emission fields. The fire started at 5 pm on February 9th. Concentrations of up to 2000 μg m^{-3} are predicted for Morwell South, the town closest to the fire. Due to the coarser resolution of the regional model, it is expected that concentrations will be lower than the near-field predictions described earlier as the averaging takes place over a larger area (i.e. 1 km compared to 100 m). The highest concentrations of $PM_{2.5}$ were predicted on 10th February at Morwell South, Churchill and Moe, which was in the initial phase of the fire. However the highest concentrations at Morwell East and Traralgon were predicted on 14th February. The model misses peak observed $PM_{2.5}$ on 21st February at Morwell South.

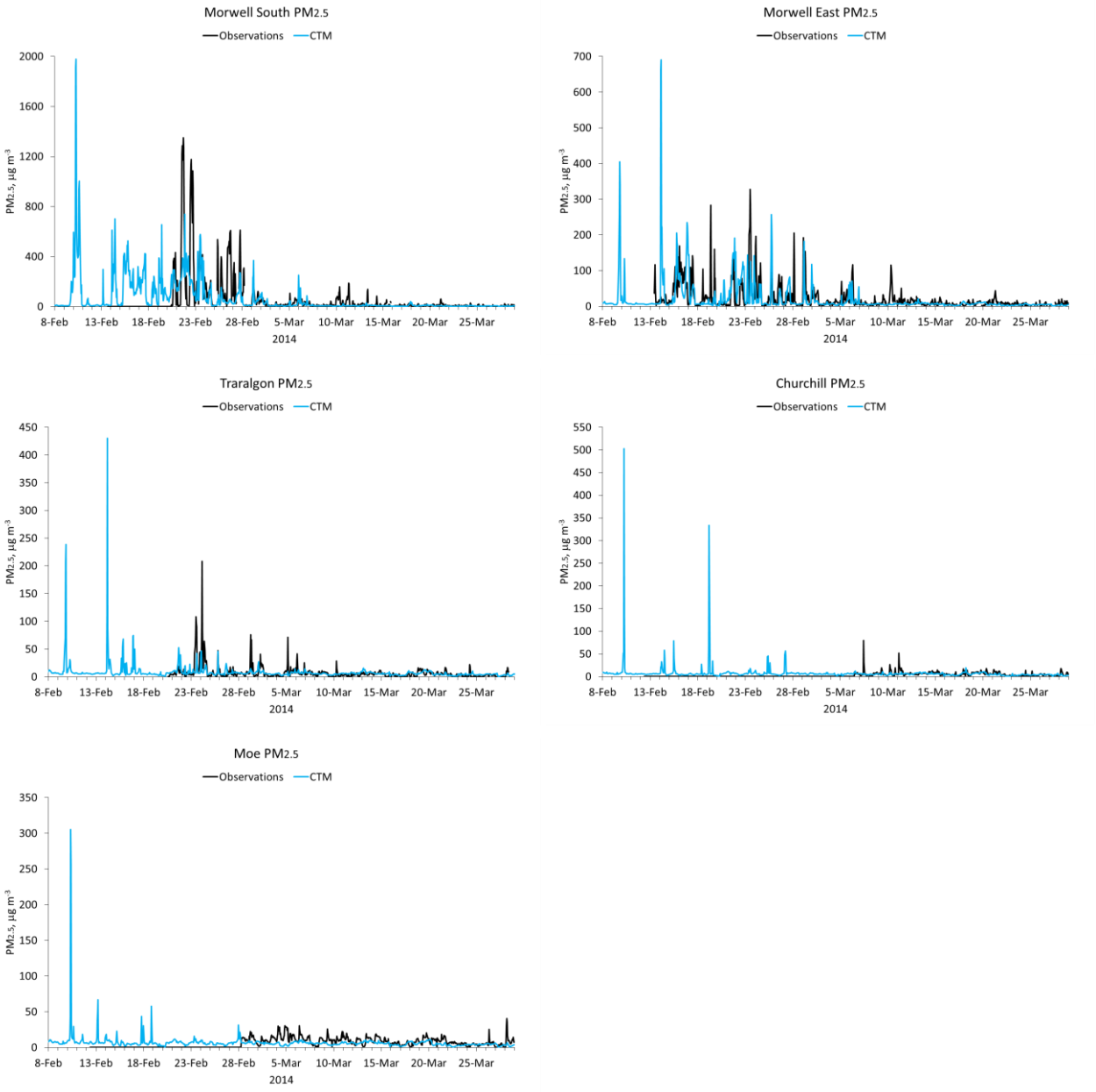

Figure 19 Time series of hourly observed $PM_{2.5}$ compared with predicted $PM_{2.5}$ from the mine fire run. Note, y-axes are not the same in each plot.

The shape of the plume on 10th and 21st February is shown in Figure 20. These maps show the spatial extent of the plume over 24 hours at the start of the mine fire on 10th February and on 21st February. The first division on the colour bars is set to 25 µg m^{-3} which is the 24 hour air quality standard for $PM_{2.5}$. At the start of the fire the winds were predominantly towards the south west, but Churchill is included on the edge of the plume. The 21st February is when the model did not predict the observed 1300 µg m^{-3} at Morwell South. The modelled plume was densely constrained on 21st February due to light winds.

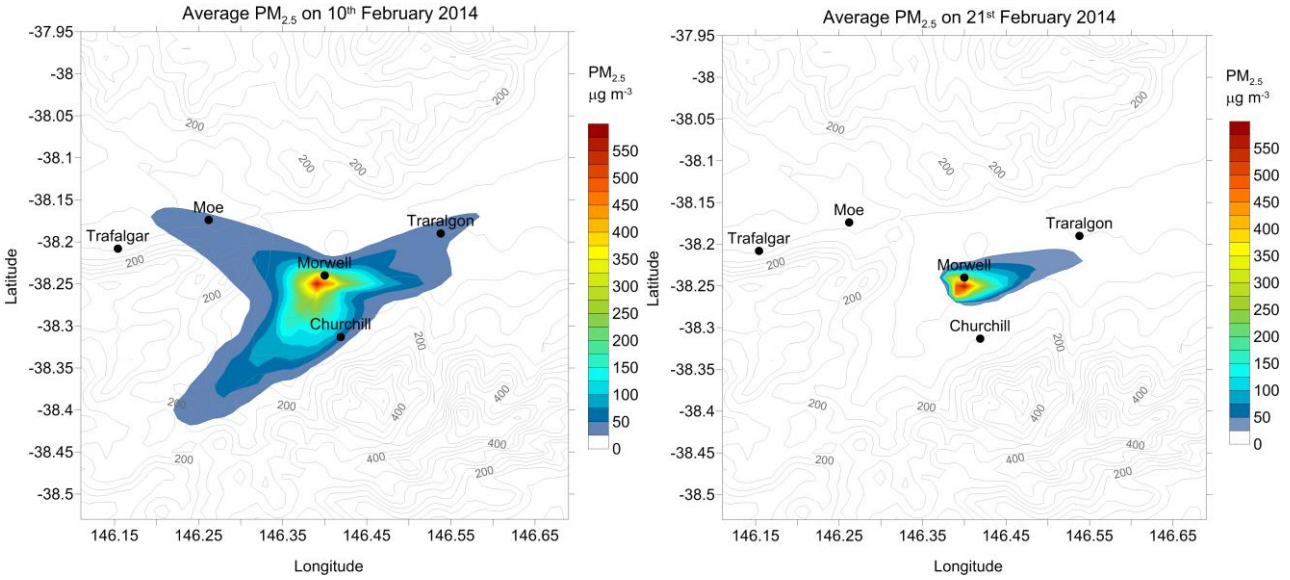

Figure 20 Maps showing average $PM_{2.5}$ concentrations predicted by the model on 10th and 21st February. Grey lines indicate topography in the Latrobe Valley.

As concentrations of $PM_{2.5}$ were highest in the initial days of the fire, it is important to analyse the predicted wind directions at this time, as measurements of $PM_{2.5}$ are not available. The dispersion of the smoke plume is dependent on predicted wind direction by the model (Figure 21). In the early phase of the fire, the wind was predominantly blowing from the east towards Melbourne. CCAM predicts wind directions swinging from 90° to ~270° on 9th February and a steady direction of ~80° from 10th until 14th February (i.e. west, away from Traralgon and Sale).

Measurements of wind direction early on in the fire are only available at Traralgon, where CCAM matches the wind direction profile very well. There are measurements of wind direction as early as 13th February at Morwell East, which also show good model to observed agreement. The good agreement in wind direction at the three sites shown gives confidence that the smoke plume is being dispersed in accordance with the observations.

The predicted concentrations of CO at the two Morwell stations and at Traralgon is shown in Figure 22. Peak CO is predicted to be 50 ppm at Morwell South on 10th February. The magnitude of the observed CO concentrations is well matched to the predictions.

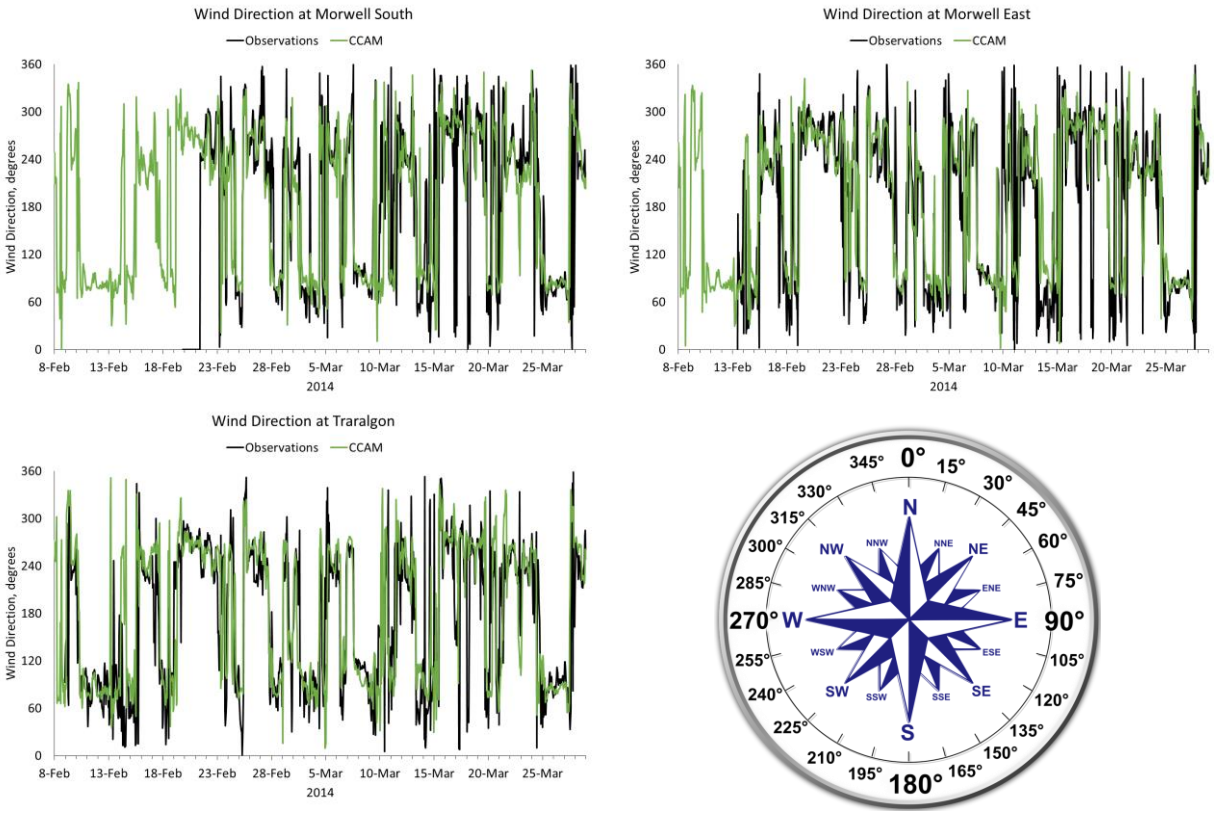

Figure 21 Modelled and observed wind directions at Morwell South, Morwell East and Traralgon. Also shown is a compass to aid interpretation. Note wind directions mean the wind is blowing from the given value.

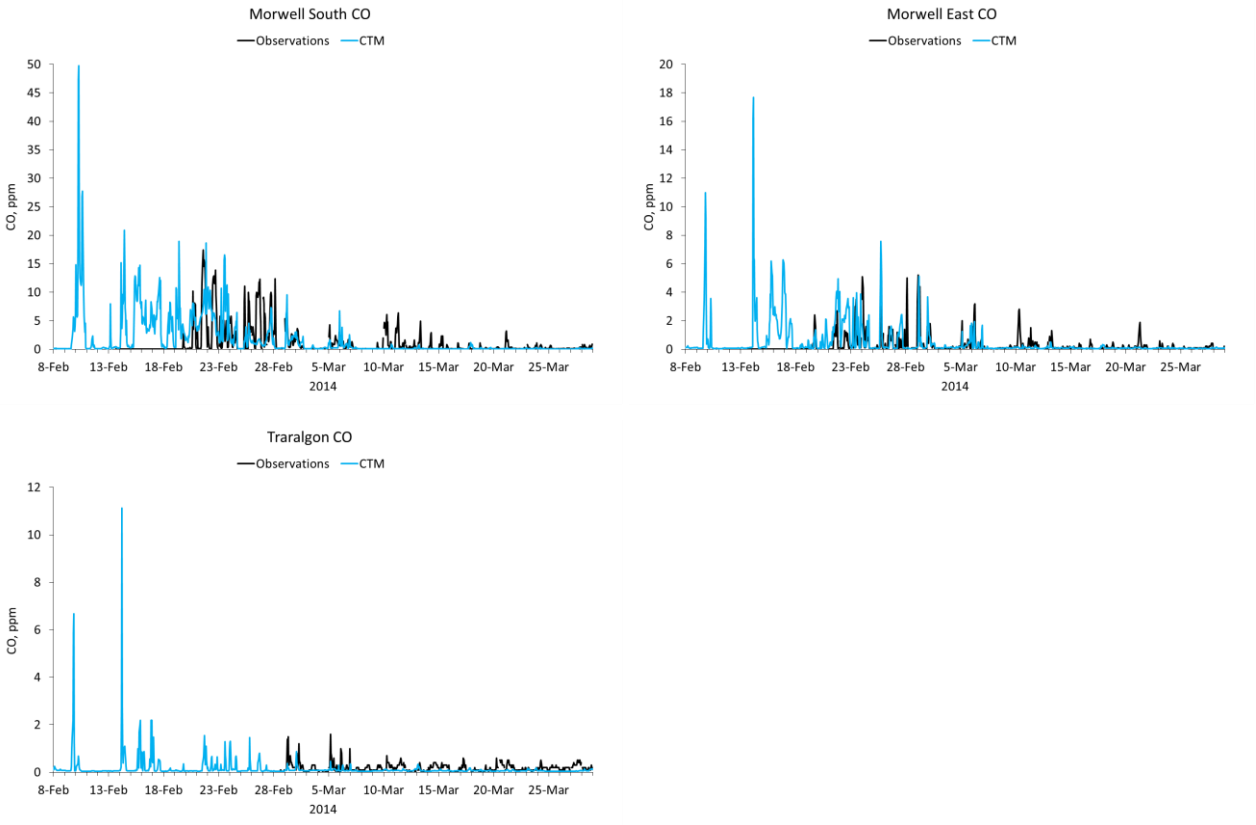

Figure 22 Time series of hourly observed CO compared with predicted CO from the mine fire run. Note, y-axes are not the same in each plot.

Maps to show the average concentration of $PM_{2.5}$ and CO over the time period of the mine fire (9th February to 23rd March) are shown in Figure 23. In both maps, the nearby towns of Morwell, Moe, Traralgon and Churchill are most impacted by smoke emissions from the fire. Leongatha, Yarram, Rosedale and Sale are not predicted to experience concentrations above the background concentrations in either $PM_{2.5}$ or CO. The effects of sea salt at the coast can still be seen in the $PM_{2.5}$ map (approx. 8 μg m^{-3} from Figure 17).

The current model run is predicting less of a geographical dispersion for the smoke at the surface as was previously predicted by the unit tracer study of Emmerson et al. (2015). The meteorological component in both runs is the same, therefore the difference is in part due to the plume rise assumption. The previous work assumed the unit tracer was emitted at 50 m; here a spatially weighted plume rise has been used from the near-field modelling, which emits the plume up to 200m in the initial stages of the fire. Thus the smoke has been transported aloft in the current run, and is more dispersed at the surface beyond 30km radius from Hazelwood.

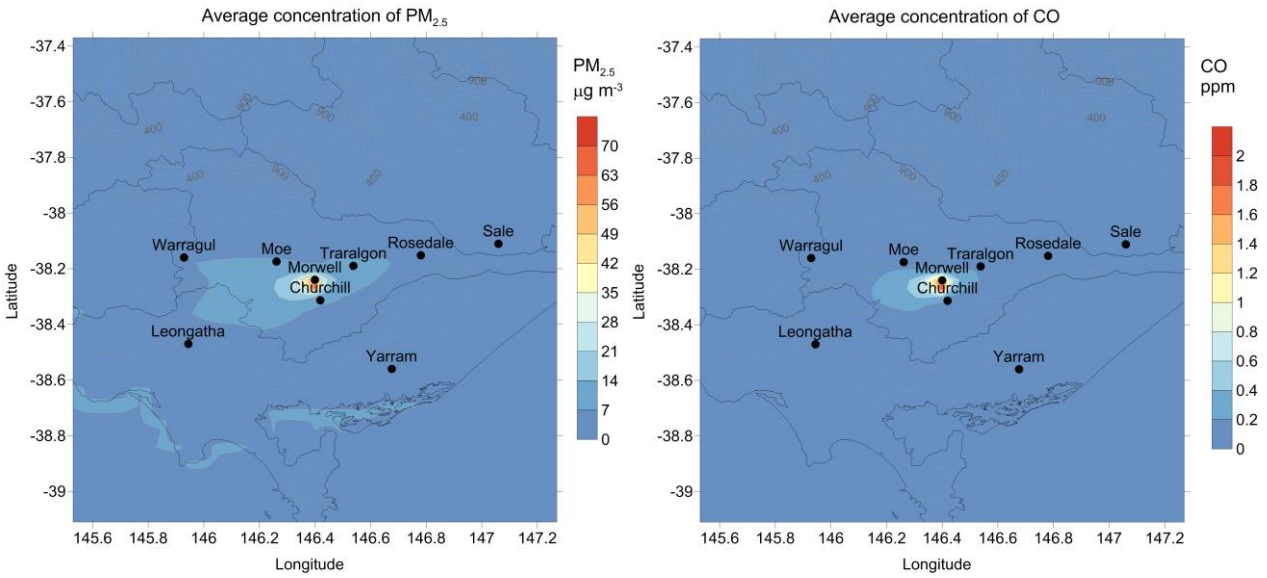

Figure 23 Maps to show predicted average $PM_{2.5}$ and CO as a result of the mine fire run across February and March 2014.

Sale was chosen as the control group for the long term health study. Figure 23 showed that the CTM has predicted low concentrations on average, of $PM_{2.5}$ (6 μg m^{-3}) and CO (0.08 ppm). Figure 24 shows the hourly concentrations of $PM_{2.5}$ and CO as predicted by the model for Sale. These predictions suggest that the presence of the mine fire did not cause any breaches of either the $PM_{2.5}$ or CO air quality standards at Sale. The peak hourly $PM_{2.5}$ concentration of 17 μg m^{-3} occurred on 10th February as the mine fire started, and the peak hourly concentration of CO (0.46 ppm) occurred on 22nd February when winds were from the west.

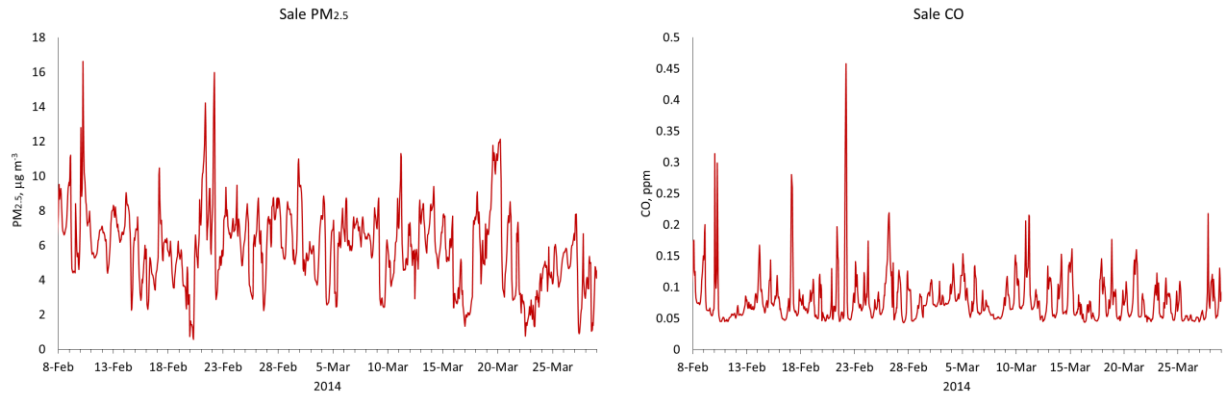

Figure 24 Time series of modelled hourly $PM_{2.5}$ and CO concentrations at Sale.

Figure 25 shows the simulated number of days on which the air quality standards for $PM_{2.5}$ and CO are exceeded on the regional scale. The 24 hour standard of 25 µg m^{-3} for $PM_{2.5}$ is used and the 8 hour average of 9 ppm for CO. At Morwell, the $PM_{2.5}$ standard is breached on 27 days, whilst for CO the standard is breached on 5 days. The CO standard is not breached anywhere else in the Latrobe Valley. At Churchill the $PM_{2.5}$ standard is breached on 3 days, whilst at Moe and Traralgon it is breached on 2 days. Despite the very high concentrations observed at these locations, the changes in wind direction mean that they did not persist for more than a few hours at a time.

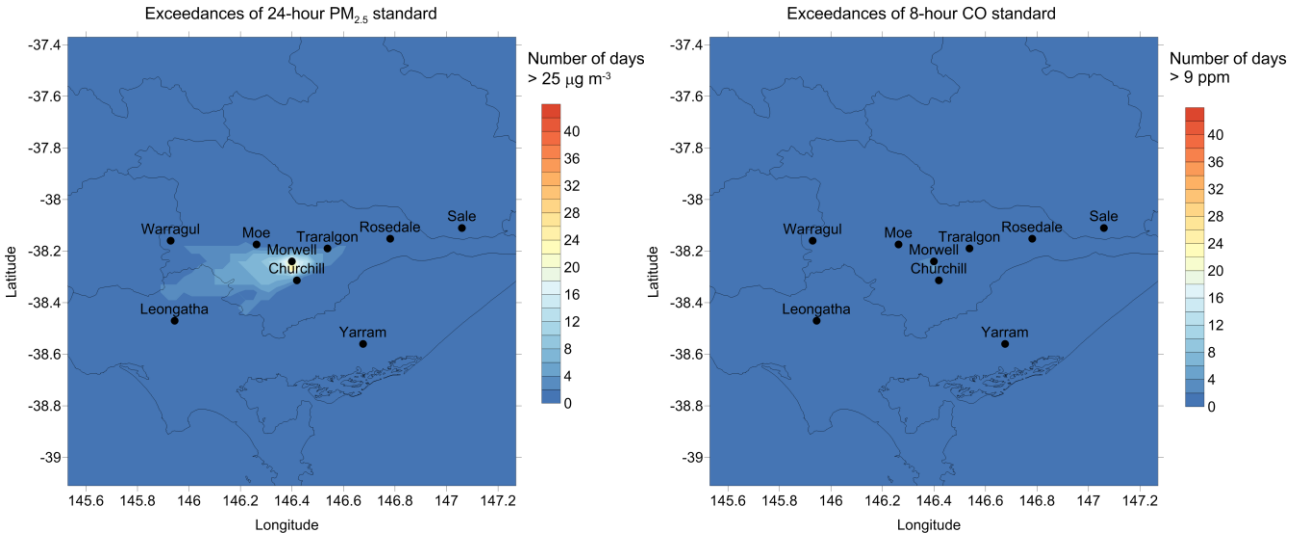

Figure 25 Spatial plots to show the modelled number of days on which the air quality standards were exceeded for $PM_{2.5}$ and CO.

5 Conclusions

CSIRO has undertaken a "bottom up" approach to calculating gridded, hourly emissions of $PM_{2.5}$ and CO from the Hazelwood mine fire. It made use of a number of parameters including daily maps of the area burned drawn by the County Fire Authority on fire activity, mass of coal burnt per unit area, hourly McArthur Forest fire danger index, and appropriate emissions factors. This emission information has been used as input to two CSIRO modelling frameworks: near-field modelling and regional modelling.

Near-field Modelling

CSIRO's TAPM model was used to simulate the near-field dispersion of the Hazelwood coal fire plume around Morwell at a horizontal resolution of 100 m. An optimised setup of the meteorological component of TAPM coupled with local wind data assimilation was used to drive the dispersion component. The coal fire area was represented by a number of ground-level point sources each 100 m apart. A mechanistic parameterisation for the rise of the fire smoke plume was incorporated into TAPM.

Background concentrations obtained from the CCAM-CTM regional model run without the coal fire emissions were added to the TAPM derived concentrations due to the coal fire emissions. The model predicts hourly-averaged peak concentrations as high as 3700 $\mu g\ m^{-3}$ for $PM_{2.5}$ and 60 ppm for CO in the early phases of the mine fire at Morwell South. These predictions for Morwell East are 2200 $\mu g\ m^{-3}$ and 35 ppm, respectively.

A comparison of the hourly-averaged modelled $PM_{2.5}$ and CO with the measurements around Morwell suggests that TAPM predicts the magnitudes of the observed concentrations reasonably well. On occasions the model does not get the observed temporal maxima at the same time with the correct magnitude, but overall, as suggested by the quantile-quantile plots in which the concentrations are considered unpaired in time, the model simulates the observed concentration distribution around Morwell satisfactorily. This result demonstrates that several assumptions made in the modelling, especially in the emissions methodology, are realistic.

The fine-scale modelling showed that residents of Morwell were exposed to the greatest number of breaches of the $PM_{2.5}$ air quality standard, exceeding it on 23 days at Morwell South and 12 days at Morwell East locations out of a total 45 days the fire burned. There were 5 breaches of the $PM_{2.5}$ limit at Traralgon. The 8-hour limit for CO was exceeded 7 times at Morwell South.

Regional Modelling

The regional CCAM-CTM model predicted background concentrations of $PM_{2.5}$ and CO in the absence of mine fire smoke emissions. This activity identified that air quality was returned to background levels in the immediate vicinity of the mine fire after March 12th (32 days after the fire started).

Peak concentrations of up to 2000 $\mu g\ m^{-3}$ for $PM_{2.5}$ were predicted in the initial phases of the mine fire at Morwell South. This was accompanied by CO concentrations of 50 ppm. These values are lower than the near-field predictions due to the coarser resolution of CCAM-CTM. Outside of Morwell $PM_{2.5}$ decreased rapidly, with peak observed concentrations at Traralgon of 342 $\mu g\ m^{-3}$. Measurements in Churchill were not made until 6th March, but the model predicted concentrations on 10th February of 503 $\mu g\ m^{-3}$. There were 3 breaches of the $PM_{2.5}$ air quality standard at Churchill, and 2 breaches at Moe and Traralgon. There were no breaches of the CO air quality standard outside of Morwell.

The regional model also predicted low concentrations of $PM_{2.5}$ and CO for the control population at Sale. The peak hourly $PM_{2.5}$ concentration predicted at Sale was 17 $\mu g\ m^{-3}$ on 10th February, whilst peak CO was 0.46 ppm on 22nd February.

References

Akagi, S. K., Yokelson, R. J., Wiedinmyer, C., Alvarado, M. J., Reid, J. S., Karl, T., Crounse, J. D., and Wennberg, P. O.: Emission factors for open and domestic biomass burning for use in atmospheric models, Atmospheric Chemistry and Physics, 11, 4039-4072, 10.5194/acp-11-4039-2011, 2011.

Andreae, M. O., and Merlet, P.: Emission of trace gases and aerosols from biomass burning, Global Biogeochem Cy, 15, 955-966, Doi 10.1029/2000gb001382, 2001.

Bandeira, J.M., Coelho, M.C., Sa, M.E., Tavares, R., Borrego, C., 2011. Impact of land use on urban mobility patterns, emissions and air quality in a Portuguese medium-sized city. Science of the Total Environment 409, 1154–1163.

Benscoter BW, Thompson DK, Waddington JM, Flannigan MD, Wotton BM, de Groot WJ and Turetsky MR (2011) Interactive effects of vegetation, soil moisture and bulk density on depth of burning of thick organic soils. International Journal of Wildland Fire 20(3), 418-429.

Bond, T. C., Covert, D. S., Kramlich, J. C., Larson, T. V., and Charlson, R. J.: Primary particle emissions from residential coal burning: Optical properties and size distributions, Journal of Geophysical Research-Atmospheres, 107, 8347-8347, 2002.

Emmerson, K., Williamson, G., Reisen, R., Cope, M., and Johnston, F.: Estimate of smoke exposure from the Hazelwood mine fire, with regards to finding a control population for ongoing health studies. CSIRO Australia 2015.

Engle, M. A., Radke, L. F., Heffern, E. L., O'Keefe, J. M. K., Flower, J. C., Smeltzer, C. D., Hower, J. M., Olea, R. A., Eatwell, R. J., Blake, D. R., Emsbo-Mattingly, S. D., Stout, S. A., Queen, G., Aggen, K. L., Kolker, A., Prakash, A., Henke, K. R., Stracher, G. B., Schroeder, P. A., Roman-Colon, Y., and ter Schure, A.: Gas emissions, minerals, and tars associated with three coal fires, Powder River Basin, USA, Sci Total Environ, 420, 146-159, 2012.

Hower, J. C., Henke, K., O'Keefe, J. M. K., Engle, M. A., Blake, D. R., and Stracher, G. B.: The Tiptop coal-mine fire, Kentucky: Preliminary investigation of the measurement of mercury and other hazardous gases from coal-fire gas vents, Int J Coal Geol, 80, 63-67, 2009.

Hower, J. C., O'Keefe, J. M. K., Henke, K. R., and Bagherieh, A.: Time series analysis of CO concentrations from an Eastern Kentucky coal fire, Int J Coal Geol, 88, 227-231, 2011.

Hower, J. C., O'Keefe, J. M. K., Henke, K. R., Wagner, N. J., Copley, G., Blake, D. R., Garrison, T., Oliveira, M. L. S., Kautzmann, R. M., and Silva, L. F. O.: Gaseous emissions and sublimates from the Truman Shepherd coal fire, Floyd County, Kentucky: A re-investigation following attempted mitigation of the fire, Int J Coal Geol, 116, 63-74, 2013.

Hurley, P., 2008. TAPM V4. Part 1: Technical Description. CSIRO Marine and Atmospheric Research Paper No. 25. ISBN: 978-1-921424-71-7, pp. 58, CSIRO, Australia.

Hurley, P.J., Physick, W.L., Luhar, A.K., 2005. TAPM: a practical approach to prognostic meteorological and air pollution modelling. Environmental Modelling and Software 20, 737–752.

Kaiser, J. W., Heil, A., Andreae, M. O., Benedetti, A., Chubarova, N., Jones, L., Morcrette, J. J., Razinger, M., Schultz, M. G., Suttie, M., and van der Werf, G. R.: Biomass burning emissions estimated with a global fire assimilation system based on observed fire radiative power, Biogeosciences, 9, 527-554, 10.5194/bg-9-527-2012, 2012.

Luhar, A.K., Hurley, P., 2003. Evaluation of TAPM, a prognostic meteorological and air pollution model, using urban and rural point source data. Atmospheric Environment 37, 2795–2810.

Luhar, A.K., Mitchell, R.M., Meyer, C.P., Qin, Y., Campbell, S., Gras, J.L., Parry, D., 2008. Biomass burning emissions over northern Australia constrained by aerosol measurements: II–Model validation, and impacts on air quality and radiative forcing. Atmospheric Environment 42, 1647–1664.

Luhar, A. K., Galbally, I. E. and Keywood, M. D., 2006: Modelling PM10 concentrations and carrying capacity associated with woodheater emissions in Launceston, Tasmania. Atmospheric Environment, 40, 5543-5557.

Luhar, A.K., Hurley, P. J., 2012. Application of a coupled prognostic model to turbulence and dispersion in light-wind stable conditions, with an analytical correction to vertically resolve concentrations near the surface. Atmospheric Environment 51, 56–66.

McGregor, J. L., and Dix, M. R.: An updated description of the Conformal-Cubic atmospheric model, in: High Resolution Numerical Modelling of the Atmosphere and Ocean, edited by: Ohfuchi, K. H. a. W., Springer, 51-75, 2008.

Meyer, C. P., Cook, G. D., Reisen, F., Smith, T. E. L., Tattaris, M., Russell-Smith, J., Maier, S. W., Yates, C. P., and Wooster, M. J.: Direct measurements of the seasonality of emission factors from savanna fires in northern Australia, Journal of Geophysical Research-Atmospheres, 117, 20305-20305, 2012.

Noble, I. R., Bary, G. A. V., Gill, A. M., 1980. McArthur's fire-danger meters expressed as equations. *Australian Journal of Ecology* **5**, 201–203.

O'Keefe, J. M. K., Henke, K. R., Hower, J. C., Engle, M. A., Stracher, G. B., Stucker, J. D., Drew, J. W., Staggs, W. D., Murray, T. M., Hammond, M. L., Adkins, K. D., Mullins, B. J., and Lemley, E. W.: CO(2), CO, and Hg emissions from the Truman Shepherd and Ruth Mullins coal fires, eastern Kentucky, USA, Sci Total Environ, 408, 1628-1633, 2010.

O'Keefe, J. M. K., Neace, E. R., Lemley, E. W., Hower, J. C., Henke, K. R., Copley, G., Hatch, R. S., Satterwhite, A. B., and Blake, D. R.: Old Smokey coal fire, Floyd County, Kentucky: estimates of gaseous emission rates., Int J Coal Geol, 87, 150-156, 2011.

Pone, J. D. N., Hein, K. A. A., Stracher, G. B., Annegarn, H. J., Finkleman, R. B., Blake, D. R., McCormack, J. K., and Schroeder, P.: The spontaneous combustion of coal and its by-products in the Witbank and Sasolburg coalfields of South Africa, Int J Coal Geol, 72, 124-140, 2007.

Poulter B, Christensen NL and Halpin PN (2006) Carbon emissions from a temperate peat fire and its relevance to interannual variability of trace atmospheric greenhouse gases. Journal of Geophysical Research-Atmospheres 111(D6), 6301-6301.

Rein, G., Cleaver, N., Ashton, C., Pironi, P., and Torero, J. L.: The severity of smouldering peat fires and damage to the forest soil, Catena, 74, 304-309, 2008.

Rein, G.: Smoldering Combustion, in: SFPE Handbook of Fire Protection Engineering, edited by: Hurley, M. J., Gottuk, D. T., Hall Jr, J. R., Harada, K., Kuligowski, E. D., Puchovsky, M., Torero, J. L., Watts Jr, J. M., and Wieczorek, C. J., Springer New York, 581-603, 2016.

Tian, L., Lucas, D., Fischer, S. L., Lee, S. C., Hammond, S. K., and Koshland, C. P.: Particle and gas emissions from a simulated coal-burning household fire pit, Environ Sci Technol, 42, 2503-2508, 10.1021/es0716610, 2008.

Urbanski, S.: Wildland fire emissions, carbon, and climate: Emission factors, Forest Ecol Manag, 317, 51-60, 2014.

Van der Werf GR, Randerson JT, Giglio L, Collatz GJ, Kasibhatla PS and Arellano AF (2006) Interannual variability in global biomass burning emissions from 1997 to 2004. Atmospheric Chemistry and Physics 6, 3423-3441.

Woskoboenko F, Stacy WO and Raisbeck D (1991). Physical structure and properties of brown coal. In 'The Science of Victorian Brown Coal: Structure, Properties and Consequences for Utilization'. (Eds R. A. Durie). pp. 152-247. (CSIRO: North Ryde, Australia).

Zawar-Reza, P., Sturman, A., 2008. Application of airshed modelling to the implementation of the New Zealand National Environmental Standards for air quality. Atmospheric Environment 42, 8785–8794.

Zhang, Y. X., Schauer, J. J., Zhang, Y. H., Zeng, L. M., Wei, Y. J., Liu, Y., and Shao, M.: Characteristics of particulate carbon emissions from real-world Chinese coal combustion, Environ Sci Technol, 42, 5068-5073, 2008.

Zonato, C., Vidili, A., Pastorino, R., De Faveri, D. M., 1993. Plume rise of smoke coming from free burning fires. Journal of Hazardous Materials 34, 69–79.

CONTACT US

t 1300 363 400
+61 3 9545 2176
e enquiries@csiro.au
w www.csiro.au

YOUR CSIRO

Australia is founding its future on science and innovation. Its national science agency, CSIRO, is a powerhouse of ideas, technologies and skills for building prosperity, growth, health and sustainability. It serves governments, industries, business and communities across the nation.

FOR FURTHER INFORMATION

Oceans and Atmosphere
Kathryn Emmerson
t +61 3 9239 4534
e kathryn.emmerson@csiro.au
w www.csiro.au

Oceans and Atmosphere
Ashok Luhar
t +61 3 9239 4624
e ashok.luhar@csiro.au
w www.csiro.au

Oceans and Atmosphere
Martin Cope
t +61 3 9239 4647
e martin.cope@csiro.au
w www.csiro.au